Surfaces of reduced and oxidized $SrTiO_3$ from atomic force microscopy

K. Szot*
Institut für Schicht-und Ionentechnik, Forschungsszentrum Jülich, D-52425 Jülich, Germany

W. Speier
Institut für Chemie und Dynamik der Geosphäre, Forschungszentrum Jülich, D-52425 Jülich, Germany
(Received 5 January 1998; revised manuscript received 6 May 1999)

Measurements by atomic force microscopy are reported for (100) and (110) surfaces of $SrTiO_3$ monocrystals prepared with different oxidizing and reducing conditions at elevated temperatures (800–1000 °C). The morphology of the surfaces turns out to be drastically altered for both oxidized and reduced crystals in comparison with the original stoichiometric surfaces. The observed changes on the surface of $SrTiO_3$ due to the applied extensive thermal treatment cannot be explained by the formation of point defects, relaxation of the uppermost surface layer, rumpling, or reconstruction due to vacancy ordering. Instead, the results have to be interpreted in terms of segregation processes and solid-state reactions at elevated temperatures which cause the formation of new chemical phases on the surface and in the region underneath. On the surface of oxygen-annealed $SrTiO_3$, this leads to the growth of steps perpendicular to the surface with step heights larger than the unit cell of the perovskite structure. Crystals prepared above 900 °C are shown to exhibit a step height of 11.8 Å which is attributed to the formation of a Ruddlesden-Popper phase $SrO^*(SrTiO_3)_n$ with $n=1$ on the surface. In the case of reduced crystals, the topographic changes on the surface are caused by the formation of Ti-rich phases such as TiO and Ti_2O on the surface above 900 °C. The complex interplay of the processes at the surface for different temperatures, in particular its dependence on the details of the heat treatment, is discussed. The induced chemical heterogeneity on the surface and in the near-surface region are interpreted in terms of a kinetic demixing. The potential driving forces for this behavior are discussed. [S0163-1829(99)09531-4]

I. INTRODUCTION

The surfaces of the perovskites of ABO_3 type are of interest for basic research as well as due to their technological applications. Of these materials, $SrTiO_3$ has attracted special attention and is generally regarded as a model substance for the perovskite group. Numerous studies exist for the surface of $SrTiO_3$ (see e.g., Refs. 1 and 2 and references therein) which have investigated the electronic structure of the stoichiometric surface (see, e.g., Ref. 3) and the influence of different types of defects (see, e.g., Ref. 4). Recent interest was stirred by theoretical results which indicate that the surface may give rise to a possible ferroelectric reconstruction[5] and may become metallic on introduction of oxygen vacancies.[6] The surface can also be of special relevance concerning the critical scattering above T_c (see, e.g., Ref. 7). Furthermore, $SrTiO_3$ was, at one time, regarded as an example case for the existence of localized surface states of *d* character,[8] which may play an important role in chemisorption properties and photolysis. $SrTiO_3$ is a particularly useful material for surface studies since it does not exhibit a domain structure which influences the topography of the surfaces; it is paraelectric and maintains the simple cubic crystal structure for a wide temperature range. Nowadays, the surface of $SrTiO_3$ has become of potential technological use as substrate for the high-T_c superconductors (see, e.g., Ref. 9 and references therein) or as part of high T_c-based heterostructures.[10]

The surface and the region below, which is sometimes called ''surface layer,'' strongly influence the macroscopic properties of $SrTiO_3$, such as the electrical conductivity[11] or dielectric phenomena at elevated temperatures.[12] It is well known that the surface region exhibits drastically different behavior compared to the bulk of the crystal. Yet the character of this region is not well understood, and there are no clear ideas about the dimension of it. It has, however, become clear that this region is not restricted, as the terminology surface layer may suggest, to the uppermost monolayers of the crystals but extends considerably into the bulk, ranging from just a few nm to even several hundreds μm. A prominent example of the disturbing effects of this region are the experiments in conjunction with the superconducting properties of reduced $SrTiO_3$.[13] It has been reported (see, e.g., Ref. 14) that a considerable amount of material had to be removed from the samples under investigation after thermal preparation before adequate experiments could be performed. The same holds true for standard electrical characterization of reduced samples (see, e.g., Ref. 15). Understanding the electrical behavior of the surface region and the character of the surface is also essential since measurements of the conductivity lie at the heart of defect chemistry and its analysis of the defect concentration (see, e.g., the recent review by Ref. 16). For this, a detailed analysis of the real surface structure and the properties at the electrode/crystal interface is necessary. In addition, the phenomena related with the surface region are of special relevance for the technological application of thin layers based on $SrTiO_3$, in particular, as a possible dielectric material for microelectronics.

Recently, microanalysis in combination with x-ray diffraction has revealed that the near-surface region of $SrTiO_3$ extending several tens of nm into the bulk of the material

develops chemical inhomogeneities after standard thermal treatment for reducing as well as oxidizing conditions.[17] This restructuring of the surface region is caused by a dramatic redistribution of material and the formation of nonperovskite phases at elevated temperatures, such as Sr-enriched phases of the so-called Ruddlesden-Popper type[18] and various forms of titanium oxides. These results shed light on the character of the real surface of $SrTiO_3$ after thermal treatment. One has therefore to ask how the restructuring of the surface region manifests itself on the surface.

The (100) surface of $SrTiO_3$ is well suited to address this question. It is the most thoroughly studied surface for the perovskites.[1,2,19,20] In an idealized description for the stoichiometric crystal, this nonpolar surface is considered to be terminated by two forms of undisturbed surface layers, the SrO and TiO_2 planes. Experiments suggest that these surfaces relax slightly perpendicular to the surface.[21] Normally, the vacuum-fractured surface exposes fragments of both types of surfaces, but special treatment can provide atomically smooth surfaces of either type.[22] For thermally reduced crystals the creation of point defects, predominantly oxygen vacancies, was taken into account and extensively investigated.[1,4] Also, the possibility of reconstruction due to ordering of the vacancies has been discussed, and both experimentally[23–26] and theoretically[6] examined. A wide range of possible reconstructions have been observed, but no consistent picture of the effects of thermal treatment under reducing conditions has so far emerged. In fact, the details of the organization of the oxygen vacancies on the surface seem to be highly dependent on preparation conditions.[25,27] Other studies have indicated an even more dramatic influence due to the thermal process. Beside the expected surface reduction with a loss of oxygen, segregation processes can lead to a change in the cation:cation ratio,[28,29] i.e., enrichment or, alternatively, depletion of either Ti or Sr. The experimental facts are, however, contradictory: whereas, according to Hirata *et al.*,[30] the (100) surface annealed in vacuum is depleted by SrO and becomes covered by only TiO_2 planes, Liang and Bonnell[28,29] (see also Ref. 31) observed an enrichment of SrO. Even more, in the study by Liang and Bonnell[28,29] the ordering on the surface as deduced from scanning tunnel microscopy measurements was tentatively attributed to the formation of the so-called Ruddlesden-Popper phases.[18] This observation points to dramatic effects at elevated temperatures and it is tempting to relate these to the above-mentioned restructuring of the near-surface region. Note that these phenomena of the reduction process do not only apply to $SrTiO_3$ but also manifest themselves in the case of a ferroelectric perovskite such as $KNbO_3$.[32]

It is thus apparent for thermal reduction that the behavior of the (100) surface of $SrTiO_3$ cannot be described by a standard point defect model in terms of only oxygen vacancies. This situation also applies to oxidizing conditions. Though much less is yet known about the effects of oxidizing conditions at elevated temperatures for $SrTiO_3$-surfaces, existing experimental observations for the (100) surface indicate a similar variety of phenomena: different forms of reconstructions and superstructures (see, e.g., Refs. 33–35), surface segregation of Sr (see, e.g., Ref. 36), as well as a large scale rearrangement of atoms giving rise to a growth of terraces.[34,37–40] The latter phenomenon causes a flattening of the surface and finds, in fact, practical importance in the use of $SrTiO_3$ as substrate for film deposition. Special interest in the rearrangement of atoms on $SrTiO_3$ surfaces has arisen in connection with the topographical changes observed on a (305) surface,[41] which makes this very special surface well suited to select optimal surface probes for atomic force microscopy. By turning to the x-ray-diffraction data[42] and microanalysis[17] of $SrTiO_3$ heat treated in oxidizing conditions it becomes apparent that, just as in the case of reduction, the whole near-surface region is affected by a major restructuring leading to a chemical inhomogeneity. Therefore dramatic changes in the morphology of the surfaces are indeed to be expected.

Our main goal in this study is to correlate the changes in the morphology of the real surface of $SrTiO_3$ after extensive thermal treatment with the restructuring observed in the near-surface region. We are taking a systematic approach by investigating the surface of $SrTiO_3$ for both reducing and oxidizing conditions prepared at different temperatures. For the surface analysis we employed mainly atomic force microscopy (AFM) to be able to study the morphology of the surfaces independent of the electrical properties of the samples. For comparison, we also performed measurements of reduced crystals with scanning tunnel microscopy (STM). We included in our investigation crystals with both (100) and (110) surfaces in order to compare the changes on the surfaces as a function of orientation.

II. EXPERIMENTAL DETAILS

For our measurements we used commercially available monocrystals of $SrTiO_3$ with (100) and (110) orientation. All the samples were grown by the Verneuil method, yet originated from different distributors (MaTecK, CrysTec). Rocking curve data provided by the manufacturer show absence of mosaic structure. The purity level was determined by chemical analysis revealing that the main contribution of impurities stems from Ba for both crystals with several dozen ppm, whereas all other impurities turned out to be well below a few ppm. For our surface analysis we used several instruments. The majority of AFM measurements were conducted at air employing a commercial instrument by Nanoscope in the tapping mode. An instrument by Omicron was also available for *in situ* experiments with AFM in the contact mode under ultrahigh vacuum conditions. We have convinced ourselves that samples prepared at high partial pressure of oxygen and under ultrahigh vacuum conditions reveal the same topographical results independent of performing the experiment *in situ* or *ex situ*. But, the latter instrument also provided the opportunity of STM measurements under the same experimental conditions. Furthermore, in some cases we also utilized a Besocke-type STM instrument.

The surfaces of our crystals showed a microroughness of the order of 1.5 nm, with a typical picture as in Fig. 1 of the (100) and the (110) surfaces, respectively. As can be taken from Table I, the (100) surface exhibited regular steps of the height of half (1.9 Å) and a full unit cell (3.9 Å), just as expected.[22,28] On higher resolution, the rugged character and bulging shape of these steps is discernible as a result of the mechanochemical preparation.

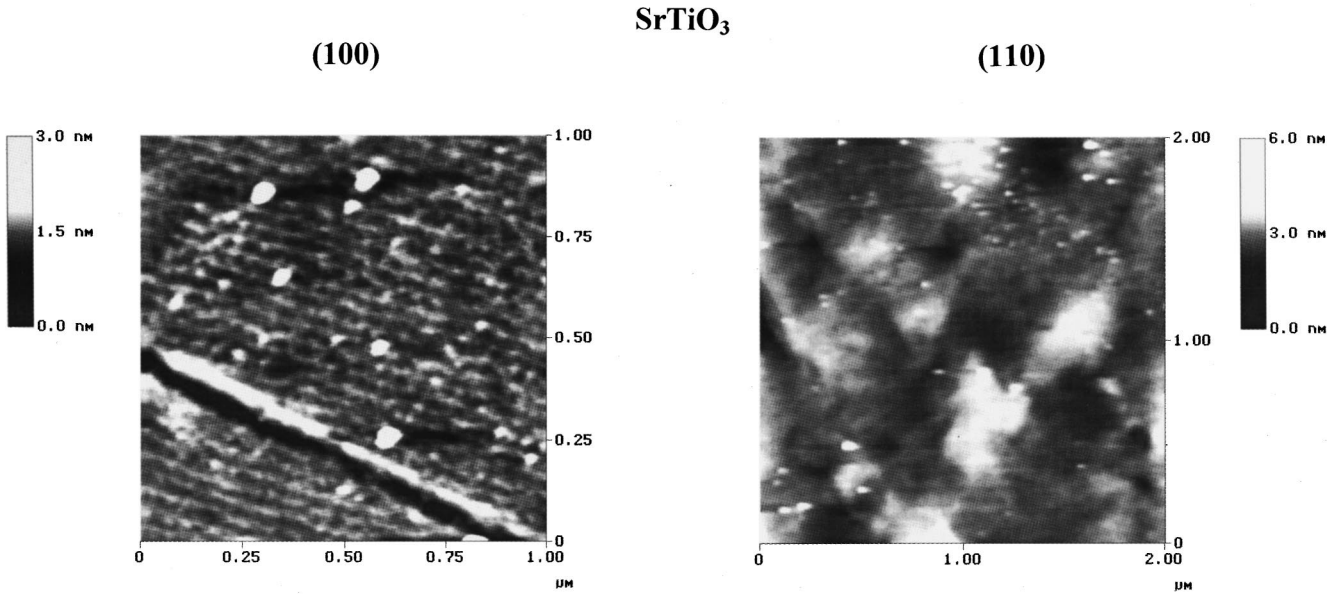

FIG. 1. AFM images of the (100) and (110) surfaces of the original stoichiometric crystal prior to heat treatment.

The traditional picture of conditioning $SrTiO_3$ crystals at elevated temperatures is based on the defect chemistry in terms of statistically distributed point defects. The preparation of our crystals at elevated temperature was therefore performed on the basis of the standard defect chemistry diagram in order to allow a direct comparison with the classical point defect models. Preparation conditions were chosen to obtain crystals in the so-called *n* and *p* regime as illustrated in Fig. 2 (Ref. 16; data for $SrTiO_3$ are taken from Ref. 43). For this, the crystals were annealed at low oxygen partial pressure ($p_{O_2}=10^{-8}$ Torr, $T=750-1000\,°C$, $t=24\,h$) and were exposed to high partial oxygen pressure ($p_{O_2}=200$ Torr, $T=750-1000\,°C$, $t=24\,h$), respectively. In this temperature range the amount of material loss is considered to be negligible.[44,45] The selected conditions also provided a direct extension of our previous study by use of x-ray diffraction (XRD) and secondary ion mass spectrometry (SIMS),[17] where we used samples from either the same batch or, at least, from the same manufacturer. SIMS allowed to check that the impurity concentration did not change in the surface region after thermal treatment.

Since the AFM and STM measurements could not be performed at elevated temperatures, we do, of course, not get an immediate picture of the surfaces *in status nascendi.* In most cases, we took care to provide an immediate heating as well as rapid cooling *in situ* (flash cooling by quenching, for reduced crystals approximately (app.) 500 °C/min and for oxidized crystals about 1000 °C/min) in order to expose the samples directly to the relevant elevated temperature and freeze the resulting surface topography, respectively.

III. RESULTS

In Fig. 3 we present results of our AFM measurements for the (100) surface of $SrTiO_3$ prepared at various temperatures under oxidizing [Fig. 3(a)] and reducing [Fig. 3(c)] condi-

TABLE I. Analysis of observed step heights of terraces on (100) surfaces for crystals heated in oxidizing conditions for different temperatures. Also included are the values for surfaces reduced at 1000 °C. All the values have been obtained by a standard averaging procedure provided by the manufacturer (Nanoscope). Two or three locations on the surface have been selected at random to analyze 10 steps in the case of oxidation and 20 steps in the case of reduction. The accuracy of step-height analysis is of the order ±0.1 Å.

Preparation conditions						
$SrTiO_3$ (100) stoichiometric	1.9 Å (40%)	3.9 Å (50%)				
$SrTiO_3$ (100) 800 °C, 200 Torr O_2, 24 h	1.9 Å (20%)	3.9 Å (30%)			5.9 Å (40%)	
$SrTiO_3$ (100) 900 °C, 200 Torr O_2, 24 h		3.9 Å (20%)			5.9 Å (30%)	11.8 Å (30%)
$SrTiO_3$ (100) 1000 °C, 200 Torr O_2, 24 h					5.9 Å (10%)	11.8 Å (80%)
$SrTiO_3$ (100) 1000 °C, 10^{-8} Torr O_2, 24 h			4.1 Å (30%)	4.8 Å (60%)		

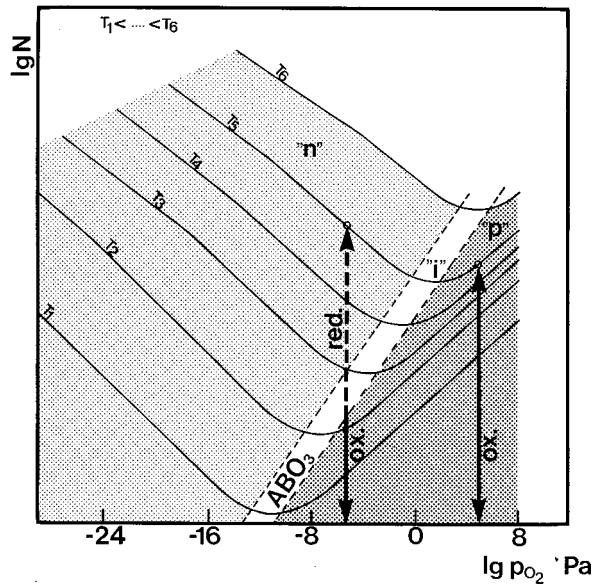

FIG. 2. Chemistry diagram for $SrTiO_3$ adapted from Ref. 43 with the concentration of defects (in arbitrary units) versus partial pressure of oxygen in Pa. The different regimes for *n*- and *p*-type $SrTiO_3$, i.e., reduction and oxidation, are indicated. The arrows denote the effect of *in-situ* heating and cooling of the samples. Note that the equilibrium position for reducing conditions traverses both *p*- and *n*-type region on heating and cooling.

tions. For comparison, the surfaces with (110) orientation are included for the oxidizing situation [Fig. 3(b)]. All the surfaces prepared at elevated temperature differed obviously drastically from the original surface with its regular arrangement of steps due to the different atomic layers of the crystal (compare with Fig. 1). The surfaces of the oxidized crystals with (100) orientation showed regular terraces of variable form and size, clearly discernible already at 800 °C. With increasing temperatures these terraces became more pronounced and exhibited sharp contours, in agreement with the literature (see, e.g., Ref. 38). Furthermore, steps of height larger than the regular perovskite unit cell (3.9 Å) were discovered, already apparent at 900 °C. At 1000 °C the size of the terraces was further enlarged and the step height turned out to be dominated by app. 11.8 Å [see also Fig. 4(a),(b)]. The detailed analysis of the step heights for different preparation temperatures can be taken from Table I. One also observes clear-cut ends of the terraces for both 900 and 1000 °C, sometimes leading to a zigzag-type structure. Finally, AFM measurements under UHV conditions in the horizontal force mode provided atomic resolution [Fig. 4(c)] and revealed that the flat areas on the terraces showed the typical lattice parameters of $SrTiO_3$ ($a=b=3.9$ Å) with an orientation of (100). It should be stressed that these results show for the first time AFM data with atomic resolution of $SrTiO_3$ surfaces, in contrast to previous results, which only allowed to determine the distance between atomic rows on stoichiometric surfaces.[37,46]

We repeated the analysis for about a dozen different crystals prepared with similar preparation conditions and always observed similar kinds of topographical changes. Only the time for these features to develop and the spatial arrangement varied from crystal to crystal. We have not performed a systematic analysis of the trends, but the existing data suggest that the individual variations depended critically on the quality of the crystals such as the impurity concentration and density of extended defects.

The oxidized crystals with (110) orientation, in particular for 900 and 1000 °C, showed a different, irregular behavior compared to the surface with (100) orientation. One can still distinguish the terracelike structure, but with decreased dimension and of correspondingly much higher density. Obviously, these terraces could not form in the same continuous manner as for the (100) surface. But still, these terraces exhibited a similar kind of characteristic concerning the step height as in the case of the (100) surface, with a dominant contribution at high temperatures (900 and 1000 °C) of steps with a height of app. 11.8 Å. On the other hand, several other fascinating features are visible on the (110) surface which indicate a different kind of restructuring as for the (100) surface. For instance, huge, roundish ridges were discernible which reminded us of a rooflike structure as visualized in Fig. 5. These features became more pronounced with increasing temperature. Furthermore, crystallites accompanied by craterlike structures developed at various, randomly distributed positions of the surface. The crystallites were much higher (e.g., 100 nm) than any of the terraces (app. 11.8 Å). The surroundings of the crystallites also showed a spiral-like ordering of terraces.

Turning to the reduced crystals, the modified surfaces [see Fig. 3(c)] gave yet another picture. Still, the surface was covered by the steplike structures of the original stoichiometric surface, but full of holes. The depth of these holes corresponds to the original step height, thus exposing the surface of the underlying atomic layer. With increasing temperatures, these holes simply grew with a rectangular, meanderlike shape at 900 °C and a mosaiclike structure at 1000 °C. Notice that, at the same time, the step height increased with temperatures. Whereas for 900 °C the major step height was still 3.9 Å, we found for 1000 °C a dominant contribution from steps ranging in height between 4.1 and 4.8 Å (see Table I). Closer inspection of surfaces for samples, which differ only in the duration of high-temperature annealing, suggest that, at first, holes appear on the surface which, then, seem to grow systematically. Subsequently, the surface rearranges in a manner which produces the new structures apparent in Fig. 3(c). Notice further, on top of all our reduced surfaces, one discovers a distribution of dropletlike features of variable size (compare also Refs. 25 and 28) and that these were almost completely absent for oxidized crystals.

In Fig. 6 we show measurements of the (100) surface of reduced $SrTiO_3$ crystals obtained by STM. The samples in this experiment had been cooled slowly under UHV conditions relying solely on the cooling rate governed by the decrease of the temperature within the oven and the heat capacity of the sample holder. This is in contrast to the measurements described above (resulting in the AFM images given in Fig. 3), where instantaneous cooling of the samples was applied by quenching, thus freezing more or less instantaneously the topographical structures on the surface. Comparing the surfaces in Fig. 6 with the AFM images in Fig. 3 reveals that the details of the experiments influenced drastically the restructuring on the surface. The surface resulting after slow cooling of the sample showed a canyonlike struc-

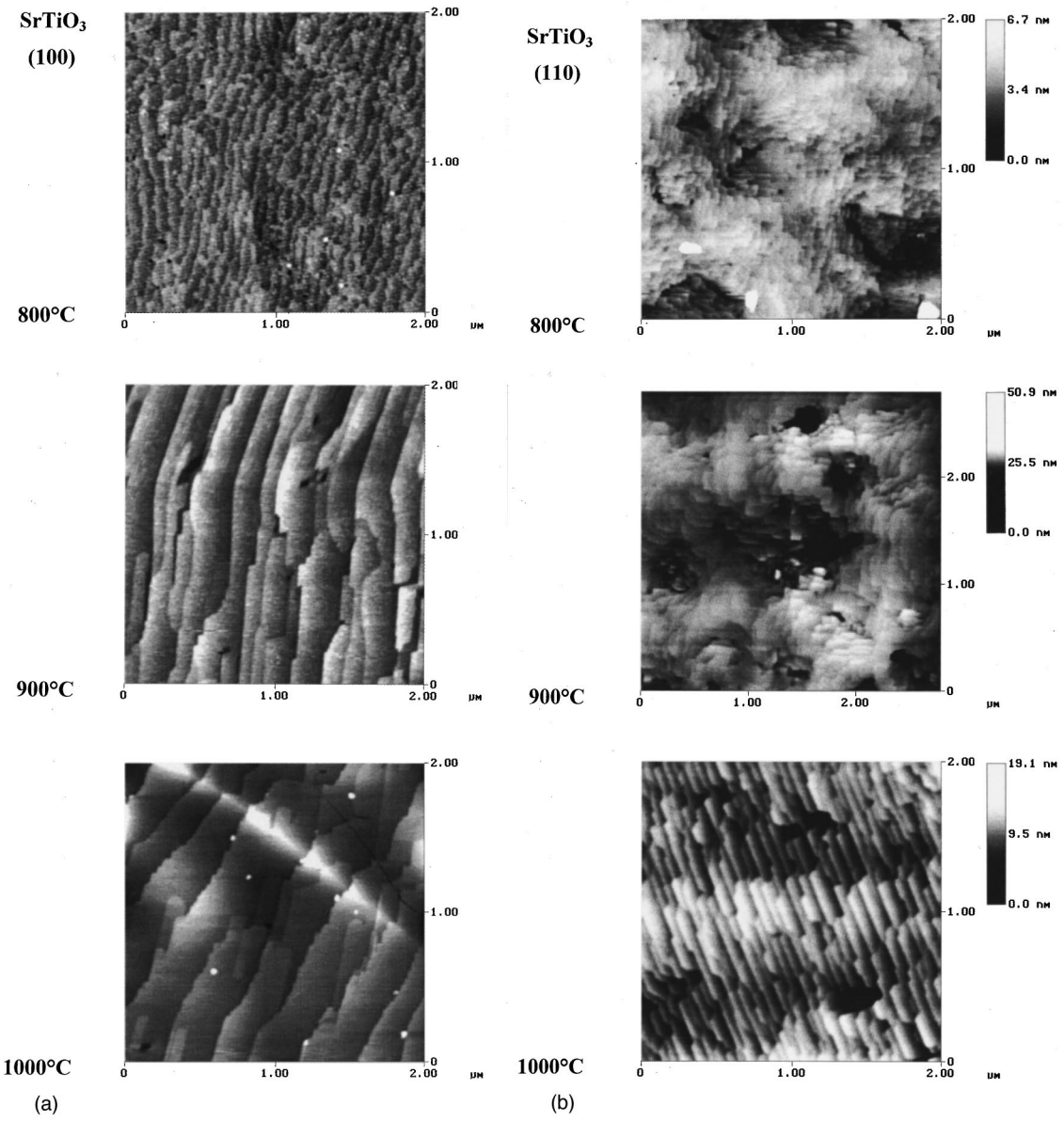

FIG. 3. AFM images of (100) surfaces after thermal treatment at various temperatures for oxidizing (a) and reducing (c) conditions. For comparison, the (110) surface oxidized with the same parameters is shown in (b).

ture. This compares well with the results of Liang and Bonnell,[28,29] except for the distance between the ridges, which turned out to be larger in our case. In order to provide an explanation for these features, we performed AFM measurements for the same kind of experimental conditions. Figure 7 shows the AFM images for different annealing times taken directly after cooling slowly *in situ*, which reveal the buildup of ridges on top of the surface. Furthermore, these experiments illustrate the development of these structures since the AFM images in Fig. 7 are obtained by successive annealing of the same sample. One can see that insular features develop at first [Fig. 7(a)]. The density of the ridges turned out to increase with time [Fig. 7(b)] and further annealing produces the canyonlike structure observed by STM as given in Fig. 6. Interestingly, the shape of the structures in Fig. 7 seems to indicate that the ridges, for these preparation conditions not yet fully established, may, in fact, have something to do with the dropletlike structure observed on the rapidly cooled samples [Fig. 3(c)]. The STM experiments, moreover, gave the opportunity to scan the top of the ridges with atomic resolution. As shown in Fig. 8, we even discovered a growth spiral with separation of the atoms related to the unit cell of the perovskite structure (3.9 Å).

IV. DISCUSSION

Our study confirms that the topography of (100) and (110) surfaces of $SrTiO_3$ crystals is completely transformed after heat treatment with both reducing as well as oxidizing conditions. Our results support the idea, proposed by Liang and Bonnell for reducing conditions,[28,29] that the observed dramatic modifications of the surface cannot be related to the formation of point defects or reconstruction due to vacancy ordering, but instead have to be interpreted by the formation of nonperovskite phases. In the following we are going to relate the morphological changes on the surface to the

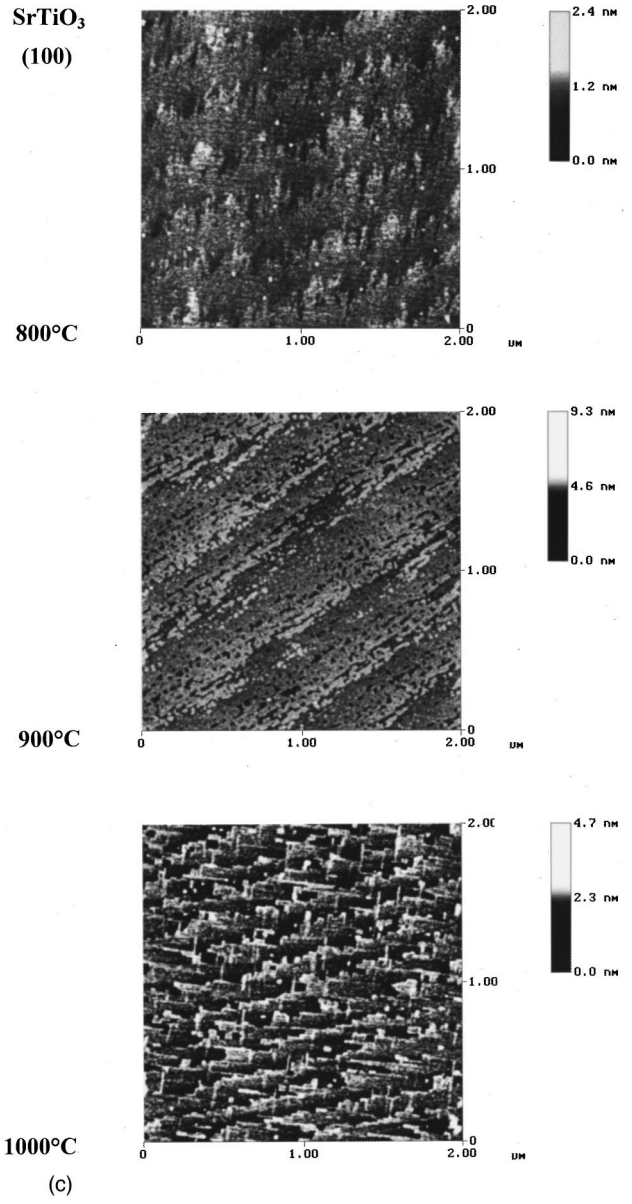

FIG. 3. (*Continued*).

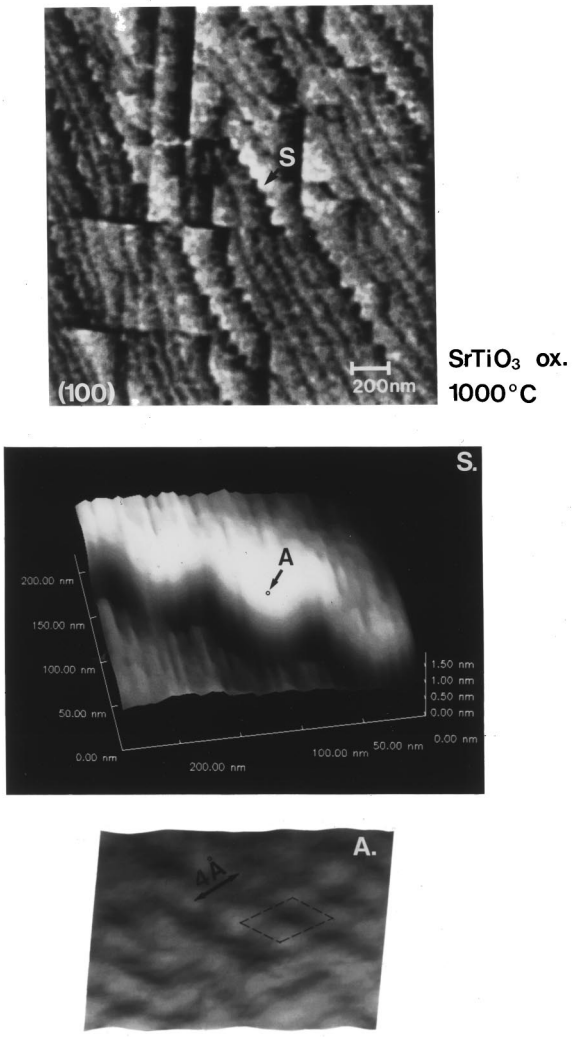

FIG. 4. Detailed pseudo-three-dimensional presentation of a (100) surface oxidized at 1000 °C [compare the upper picture also with Fig. 3(a)]. The topography has a pronounced zigzag-type structure [see details of segment S in the middle picture, (b)] and is governed by a step height of 11.8 Å. This is related to the lattice constant in the *c* direction of a Ruddlesden-Popper phase (Sr_2TiO_4) which is perpendicular to the surface. Enlargement (segment A indicated in the middle figure) reveals the perovskite unit cell ($a = b = 3.9$ Å) with atomic resolution [lower picture, (c)].

restructuring in the near-surface region of the crystals. The qualitative model developed for the complex interplay of these phenomena, presented in Ref. 17, forms the basis of our interpretation. We therefore start below with a short review of this description before entering into the detailed interpretation of our findings. We will then provide a detailed analysis of the experimentally observed changes in the surface morphology for the oxidizing and reducing conditions. Finally, we will conclude with a discussion of the possible driving forces responsible for the restructuring of the surface and the region below.

A. Induced chemical heterogeneity in the near-surface region

The standard models of defect chemistry developed to describe the bulk properties of perovskite of ABO_3 type after equilibration at elevated temperature are based on the idea that thermal treatment of the crystals leads to the occurrence of point defects within the bulk of the material (see, e.g., Refs. 16 and 47, and references therein). The basic assumption for the nonstoichiometry is thus a crystal with only a statistical distribution of point defects and their diffusion by random walk in an otherwise homogeneous crystal. The corresponding defect chemistry diagrams (see Fig. 2) relies on measurement of the so-called ''equilibrium'' electrical conductivity and its relation to the partial pressure of oxygen in the surrounding atmosphere.

However, experimental evidence suggests that the samples treated in the standard manner at elevated temperatures are, in fact, not in equilibrium. Instead, restructuring of the near-surface region leads to a continuous development of a chemical heterogeneity starting out from the surface in contact with the outer atmosphere[42] and growing into the crystal with time.[17] The corresponding chemical phases have been identified by x-ray diffraction on pulverized single

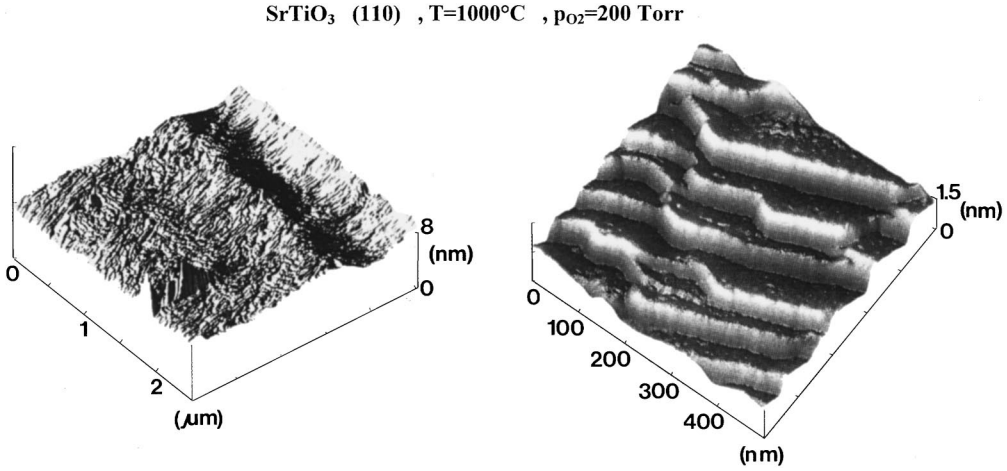

FIG. 5. Detailed pseudo-three-dimensional presentations with various enlargements of a (110) surface oxidized at 1000 °C [see Fig. 3(b)].

crystals, whereas microanalysis by secondary ion mass spectrometry of single crystals has served to monitor the in-depth redistribution of Sr and Ti. The dynamic character of this chemical heterogeneity can be directly inferred from the experimentally determined rate of formation of the nonperovskite phases in $SrTiO_3$ for different temperatures as collected in Fig. 9. The proportion of nonperovskite phases increases linearly with time (for more details, see Ref. 42), at least for the typical length of heat treatment as was also used in this work. Notice that for much longer exposure times the formation rate may change, but has so far not been investigated. Similarly, no information is yet available about the dimensions of this chemical heterogeneity for single crystals after extensive annealing.

The distribution of chemical phases within the near-surface region is schematically illustrated in Fig. 10. Notice, for the kind of thermal treatment employed in this work a region of at least 30–40 nm into the bulk of the crystals is affected by the formation of the chemical heterogeneity. In this context it should be mentioned, that our previous work was performed using, in some cases, the same crystals or, at least, crystals from the same manufacturer and with similar experimental conditions.

Taking our experimental data as a guideline, one can deduce that the restructuring for reducing conditions can be characterized by the general form

$$k\times SrTiO_3 \leftrightarrow p\times SrTiO_3 + q\times SrO(SrTiO_3)_n + s\times Ti_2O + t\times TiO + (3s+t)/2\times O_2\uparrow \quad \text{with } k=p+q\times(n+1),\ 2s+t=q. \tag{1}$$

It is important to notice that Ti_2O is actually the main Ti component observable in the x-ray-diffraction data for the preparation conditions considered in the present work. In the case of oxidizing conditions, the chemical reaction would be described in a basic form by

$$k\times SrTiO_3 \leftrightarrow p\times SrTiO_3 + q\times SrO^*(SrTiO_3)_n + q\times TiO_2 \quad \text{with } k=p+q\times(n+1). \tag{2}$$

Taking into account the full complexity of the processes involved for oxidizing conditions one would also have to include the so-called Magnéli-type structures (Ti_mO_{2m-1}, see, e.g., Ref. 48), an ordered form of oxygen-deficient TiO_2 observable in our x-ray-diffraction data,[42] as well as the possible uptake of oxygen from the surrounding atmosphere.[49]

The occurrence of the homologues series of Ruddlesden-Popper (RP) phases [$SrO^*(SrTiO_3)_n$] (Ref. 18) is a result of an intergrowth of SrO into the original perovskite-structure. On the other hand, the TiO-rich phases form by dismantling of SrO layers and, in the reduced case, by additional reduction with a loss of oxygen. It should be emphasized that due to the dynamic character of the restructuring the description of the above given reactions constitute only a spotlight on the actual processes. All variables are to be considered as time dependent and the final state of the chemical composition of the crystal is yet unknown.

The formation of Ruddlesden-Popper and Magnéli phases are well known in the literature for the SrO-TiO_2 pseudobinary system (for the RP phases see, e.g., Refs. 18 and 50–53, for the Magnéli phases see Ref. 54). It turns out that already small changes in the Sr/Ti stoichiometry for $SrTiO_3$ are sufficient to produce these phases as the excess solubility limit for both TiO_2 and SrO are known to be rather low.[55] It should be pointed out that the intergrowth of SrO layers

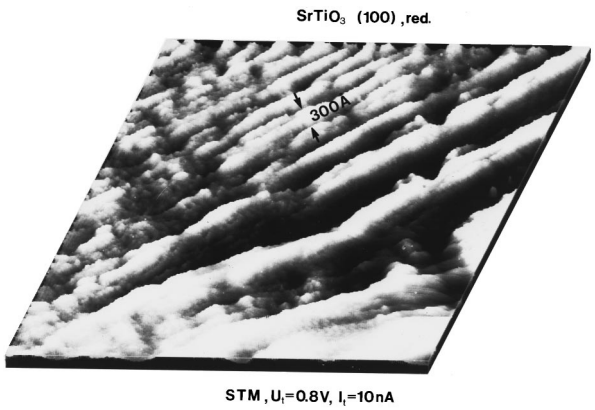

FIG. 6. STM image taken for (100) surface heated in reducing conditions and slowly cooled in UHV. A canyonlike structure is clearly visible.

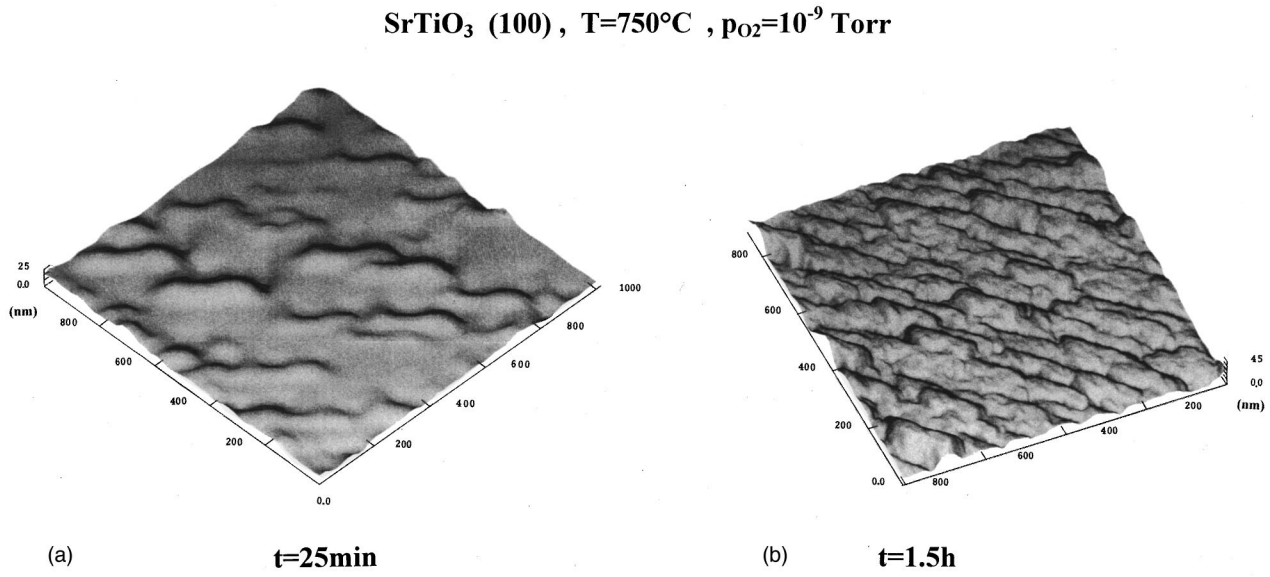

FIG. 7. AFM images taken *in situ* of a (100) surface after slow cooling of samples heated in reducing conditions to 750 °C for 25 min (a) and then reheated for 1.5 h (b).

leading to the RP phases is not necessarily in an ordered fashion, but is rather given by a random distribution leading to microregions of different compositions (see the pioneering work of Tilley),[50] i.e., varying values of *n*. Interestingly enough, the disorder can be characterized by the directional growth of perovskite lamellae with values of *n* which are both lower and higher than the nominal crystal composition. Some of the information on the microstructure of the RP phases can be set in relation to our results on the reorganization of the surface region for thermally treated $SrTiO_3$. It is thus not surprising that our x-ray-diffraction data for the oxidized crystals[42] revealed an intercalation level of the RP phase varying over a range of values of *n*, in our case from $n=1$ to 6. Recent detailed analysis even indicated that RP phases up to $n=10$ may occur.[56] Notice that only in the case of reduced crystals did we find a very limited number of RP phases, with $n=3$ being highly dominant.[17] In this context note finally that isolated planar faults caused by the intergrowth of SrO layers are known to exist in stoichiometric (disordered) $SrTiO_3$.[50]

The local chemical heterogeneity developing in the near-surface region as a result of the heat treatment forms by redistribution of Sr and/or SrO and subsequent solid-state reactions. The role of *A*O as source and sink in the formation of a local chemical heterogeneity in ABO_3-type perovskite has been set in relation to the high degree of *A*O-nonstoichiometry, the so-called γ-nonstoichiometry, in perovskites[57] well documented for the more volatile PbO in

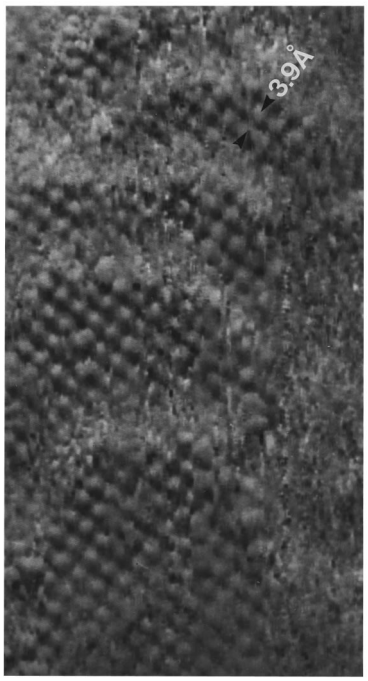

FIG. 8. STM image of a growth spiral taken on top of a ridge of the canyonlike structure of Fig. 6.

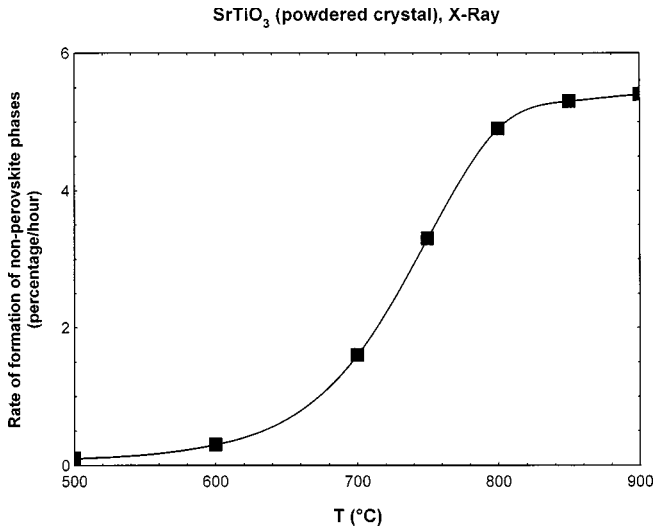

FIG. 9. Rate of formation of nonperovskite phases in $SrTiO_3$ for oxidizing conditions at different temperatures (adapted in parts from Ref. 42).

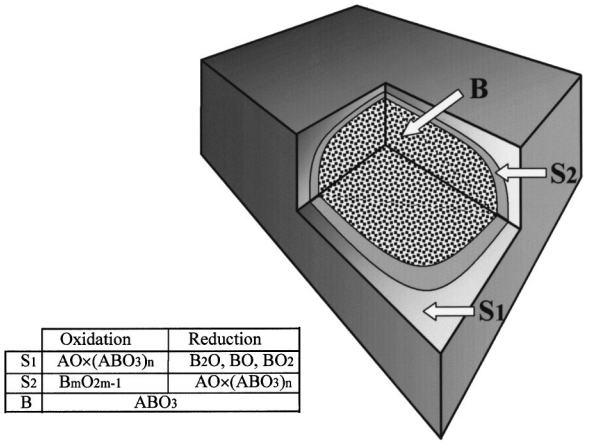

	Oxidation	Reduction
S1	$AO\times(ABO_3)_n$	B_2O, BO, BO_2
S2	B_mO_{2m-1}	$AO\times(ABO_3)_n$
B	ABO_3	

FIG. 10. Schematic illustration of the chemical heterogeneity in the surface region of a $SrTiO_3$ crystal induced by oxidation or reduction at elevated temperatures.

$PbTiO_3$ or $PbZrO_3$ (see references in Ref. 57). It should be stressed that the range of temperatures involved in our experiment (up to 1000 °C) lies below the limit where evaporation of SrO has to be taken into account. In this respect, the redistribution of SrO within the crystal could be considered as a precursor of the general tendency of the perovskite to form the AO nonstoichiometry at high temperatures.[58] Above 1000 °C the possibility of Sr loss due to evaporation can no longer be neglected (see below). Notice, that for the easy reorganization of the chemical composition observed (already at 500 °C!), fast diffusion paths are necessary. The existence of such special transport paths due to extended defects in perovskite of ABO_3 type can be directly deduced from tracer experiments (^{18}O) with SIMS analysis ($CaTiO_3$,[59] $KNbO_3$,[32] but see Ref. 60). Furthermore, the fast reorganization of AO layers near the surface of perovskite has been observed *in situ* by transmission electron microscopy (for $Ca_{1-x}Sr_xTiO_3$ see Ref. 52, for $BaTiO_3$ see Ref. 61) and has been referred to as ''zipper effect.''[62] Of course, these results cannot be directly compared to our situation since those experiments have been performed under electron irradiation. But, the observations give an impressive account of the ease of reorganization of atomic layers in the surface region of ABO_3 perovskite and can most probably be transferred to the thermal treatment of stoichiometric $SrTiO_3$.

The restructuring in the near-surface region is obviously a complex interplay of processes with the depletion and enrichment of SrO, the role of special fast diffusion paths and subsequent solid-state reactions. Figure 11 provides a visualization of the possible combinations of these processes for one specific example case, here representing the basic reaction for oxidizing conditions as summarized in Eq. (2). The illustration sketches out the dismantling of SrO layers, transport along extended defects and subsequent intercalation in the perovskite structure. The ordered intergrowth of SrO can lead to the formation of RP phases (here only the highest level RP phase with $n=1$) and a shearing mechanism is responsible for the formation of TiO_2. The schematic illustration does not depict the full complexity of the processes involved, but is used to contrast the restructuring of the near-surface region with the standard description of defect chemistry of perovskite in terms of point defect models.

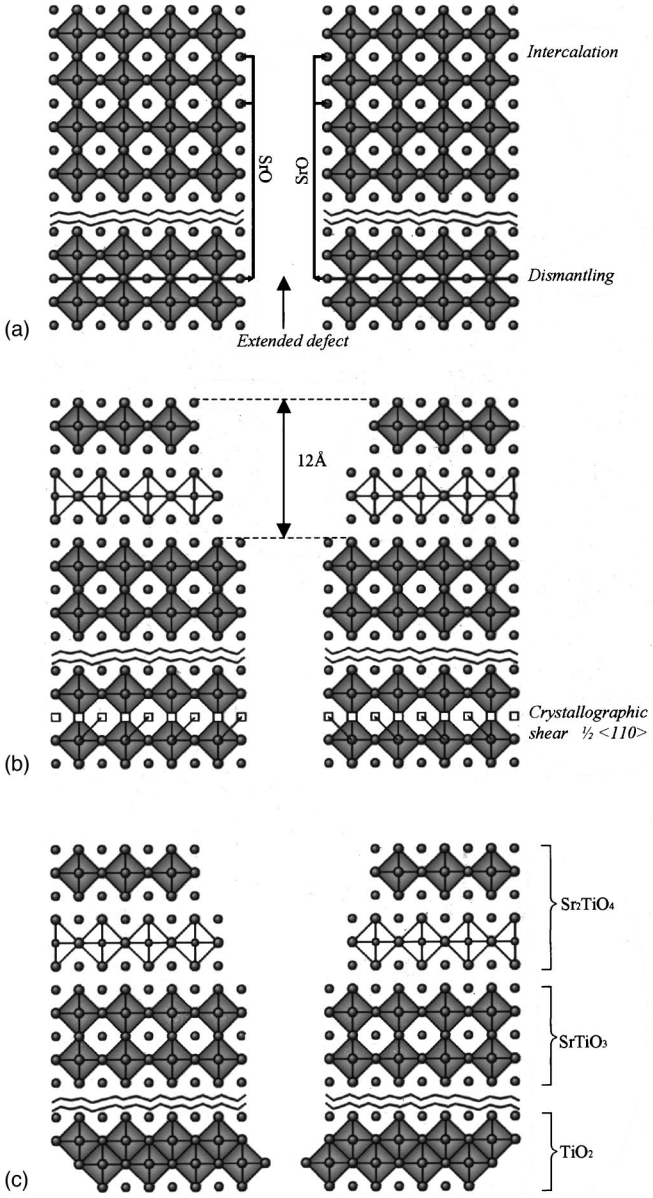

FIG. 11. Schematic illustration of the possible restructuring of the near-surface region of $SrTiO_3$ at elevated temperatures for oxidizing conditions. The figure depicts in a simplified manner the interplay of basic processes, such as dismantling, transport, and intercalation of SrO layers (a) as well as corresponding shearing mechanisms [see (b)], which result in the chemical modification of the near-surface region (c) with the formation of Ruddlesden-Popper phases (here only Sr_2TiO_4) and Ti-rich phase (here only TiO_2). The presented scheme combines information from a range of available experimental data, mainly by x-ray diffraction (Refs. 17 and 42), microanalysis (Ref. 17), high-resolution transmission electron microscopy (Refs. 50 and 79) and atomic force microscopy (this work). But note, the illustration does not reflect the full complexity of the processes (see text). For reducing conditions basically the same kind of basic processes are involved in the restructuring of the near-surface region taking into account, in particular, the continuous loss of oxygen from the surface.

The complexity of processes involved in the restructuring of the near-surface region can give rise to a variety of surface behavior. Most prominent influences are the duration of thermal treatment, the specific details of heat treatment, as well

TABLE II. Lattice constants [Å] of $SrTiO_3$, Ruddlesden-Popper phases $Sr_{n+1}Ti_nO_{3n+1}$ (space group $I4/mmm$) taken from Ref. 42.

	$SrTiO_3$	Sr_2TiO_4	$Sr_3Ti_2O_7$	$Sr_4Ti_3O_{10}$	$Sr_5Ti_4O_{13}$	$Sr_6Ti_5O_{16}$
$a=b$:	3.992	3.983	3.935	3.927	3.922	3.922
c:	3.992	11.80	19.66	27.50	35.40	43.16

as the thermal history of the samples under investigation. Further influence may result from surface preparation prior to thermal treatment such as, for example, ion bombardment. Moreover, the experimental technique itself may affect the surface as, for example, encountered in case of electron irradiation with the possibility of induced migration of surface ions (see, e.g., Ref. 63). Before going into a detailed discussion of the experimental results for the morphology of the surface, a few features of our study should be emphasized. First of all, we have applied extensive thermal treatment in keeping our samples at elevated temperatures for at least 24 h. Though considerable changes on the surface can already be observed after much shorter times (see also, e.g., Fig. 7), the extended annealing times was chosen in order to allow the restructuring in the near-surface region to be well established. Second, it turned out to be a vital ingredient to consider the specific details of the thermal treatment, in particular the effect of heating and cooling rates for reducing conditions (see discussion in Sec. IV C). Furthermore, we always used fresh (''virgin'') samples for a new set of preparation variables. This way we excluded the influence of the thermal history of the crystals as a cause for specific changes on the surface. And finally, we avoided any use of ion bombardment or flash heating for cleaning of the surface.

B. Surfaces of oxidized crystals

Considering now the AFM results, we are actually able to assign the structures on the surface of the oxidized crystals to the formation of RP phases. For this, we use the observed step-heights collected in Table I. The regularity of the experimental values cannot be related to a simple step bunching with multiples of the $SrTiO_3$ unit cell. Instead, by reference to the lattice parameters for different RP phases listed in Table II, we conclude that the terraces on the surface of the $SrTiO_3$ crystals oxidized above 900 °C originate from a RP phase with $n=1$ (Sr_2TiO_4). In this case, the RP phases of higher n identified by XRD have necessarily to be situated in deeper layers of the surface region. The experimental results of the oxidized (100) surface (see Fig. 4) can therefore be interpreted in such a way that the growth of these phases has to occur perpendicular to the surface. Whereas at lower temperatures (around 800 °C) the terraces show only a mixture of various step heights related to the unit cell of the perovskite structure, the surfaces at higher temperatures (around 900–1000 °C) are covered almost completely with steps related to the extra RP phase of $n=1$. The formation of the step-terrace structure and the continuous growth in width agrees well with recent AFM measurements by other groups.[37–40] The fact that the whole surface may be covered after extensive heat treatment with the step height corresponding to Sr_2TiO_4 is interesting. So far, only intermediate step-heights had been mentioned for much shorter annealing times.[38] But note that such a surface with well established terraces of step height corresponding to Sr_2TiO_4 may lend itself to an improvement of film deposition of high-temperature superconductors, such as $YBaCuO_4$, which has a unit cell of 11.75 Å.

TABLE III. Lattice constants of Ti_2O with space group $P\bar{3}m1$ and TiO with space group $Fm3m$ taken from Ref. 93.

	Ti_2O	TiO
a:	2.95	4.2
c:	4.85	

The enrichment of Sr close to and on the surface is a result of the segregation of Sr and/or SrO at elevated temperatures under oxidizing conditions. This has been experimentally verified for undoped $SrTiO_3$ by Auger spectroscopy (see, e.g., Ref. 36, and references therein) and SIMS analysis.[17] The effect of a continuous transport of material to the surface can even be inferred from AFM measurements. For this, we compare in Fig. 12 (100) surfaces for samples from the same crystal prepared at 1000 °C for 24 and 120 h. One can clearly see that dropletlike features [similar to the features observed in the reduced case, see Fig. 3(c) and below] become visible on the surface after heat treatment appearing along with the steplike terrace structure. At 24 h these features are still rare, but their density and size increases with time. As can be also taken from Fig. 12, the effect is dramatically accelerated at higher temperatures (here 1100 °C). In this case, even some conglomeration of the features becomes apparent. Even more, after 120 h we discovered microcrystals which have grown on top of the surface. At the same time, the droplet features have disappeared in the close vicinity of these crystals. Whereas the dropletlike features do not show any facetting, the microcrystals are regularly shaped and exhibit nicely oriented surfaces. Furthermore, the microcrystals can be shown experimentally, by elemental distribution mapping,[64] to consist almost exclusively of Sr as cationic species. Therefore just as in other studies (see below), we interpret the dropletlike features as accumulation of SrO on the surface. The results indicate that the longer the heat treatment or the higher the temperature the excess amount of SrO on the surface gets obviously not structurally accommodated. One may argue that the formation of the Ruddlesden-Popper phases at an early stage of heat treatment, in particular Sr_2TiO_4 on the surface, hinders further intergrowth of SrO at a later stage. With prolonged heating, the agglomeration of these features seem to lead to a recrystallization of the extra material resulting in the formation of microcrystals. At the same time, surfaces modified in this way also seem to lose Sr/SrO by evaporation at temperatures above 1000 °C as evident from thermogravimetrical measurements (see below). In any case,

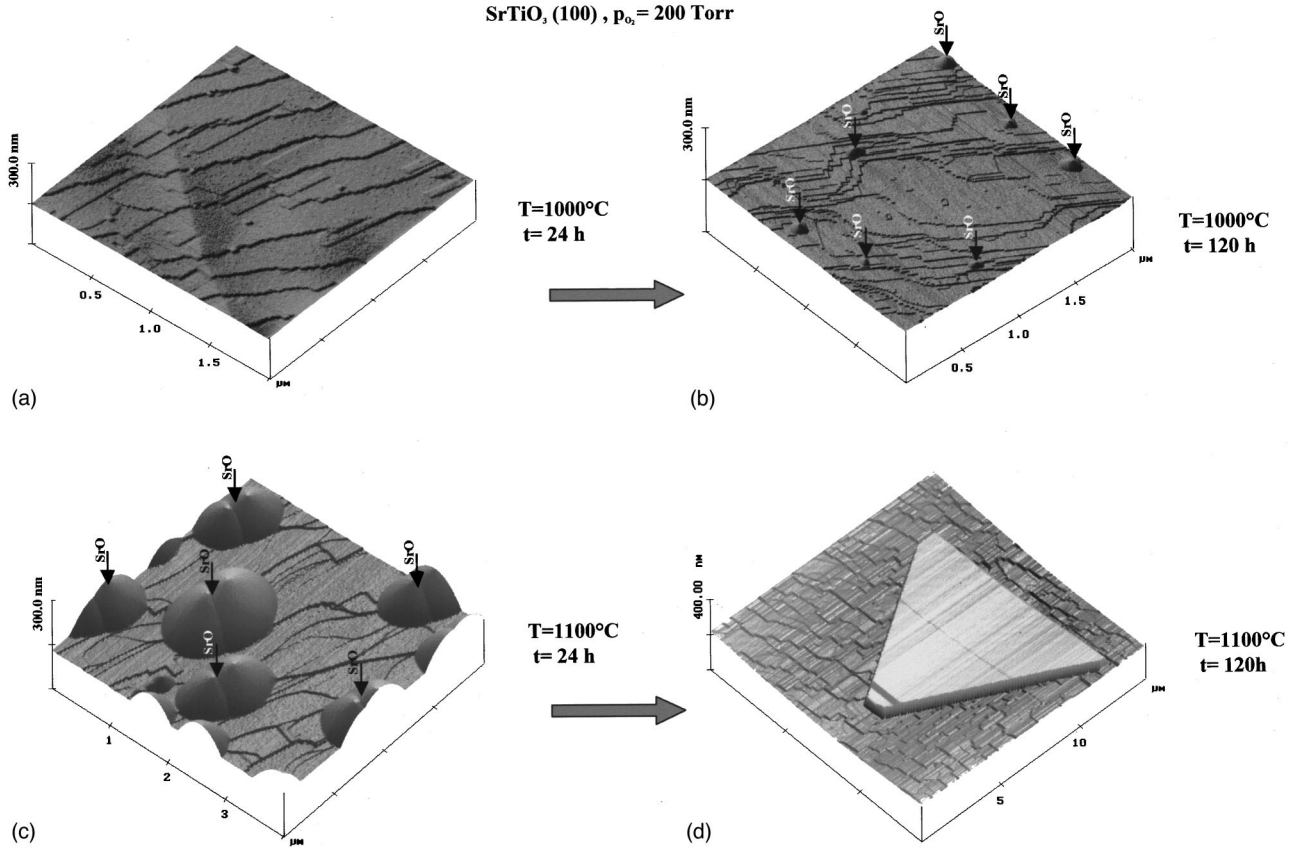

FIG. 12. AFM measurements of (100) surfaces prepared at 1000 °C for 24 h (a), 120 h (b) and at 1100 °C for 24 h (c) and 120 h (d). The data give evidence for the appearance of droplet features, which are attributed to SrO, for prolonged heating and higher temperatures. The regular microcrystal in (d) arises due to the agglomeration of the dropletlike features.

the result is an impressive account of the fact that the surface for the kind of heat treatment applied is not in equilibrium but undergoes further changes in time (see above), in this case the continuous accumulation of SrO. Notice that such a precipitation of SrO on the surface makes it also necessary to extend the description of the effect of oxidizing conditions as given above in Eq. (2) (see also Ref. 49).

The topography observed for (110) surfaces can also be understood within the suggested framework. For this, the original (110) surface should be regarded as a conglomeration of microregions, where terraces of orientation in (100) direction dominate. This can be related to a preferential fracturing along the (100) direction since this is the natural cleavage plane for the material. The new phases formed on the (110) surface do also show a preferential growth. The phases (with step size of 11.8 Å) can then be thought of as expanding the terraces with (100) orientation, growing again perpendicular to the (100) direction. This way, the observed rooflike structure can be explained as an accumulation of terraces in the (100) direction. However, the continuity of the (100) terraces, as in the case of the (100) surface, is not achieved for the (110) surface, and thus leads to the irregular growth observed.

A consistent picture emerges for the effects of oxidation of $SrTiO_3$ crystals combining atomic force microscopy with micro- and phase analysis. Our results confirm that AFM is a versatile tool to visualize the effects of the restructuring on the surface for oxidizing conditions. In this respect, the data for the (110) surfaces [see again Fig. 3(b)] provide a particularly impressive account of the extent of changes occurring at elevated temperatures.

C. Surfaces of reduced crystals

The observed topographical changes on the surface for reduced crystals were highly dependent on the experimental details. This becomes apparent by a comparison of Figs. 3(c) and 6. The differences were related above to the details of heat treatment. In this context one should note that all hitherto reported experiments of STM for reduced crystals (also in this work) have not actually been performed at elevated temperatures, but instead at room temperatures. Only high-temperature measurement (fracturing and measuring at elevated temperatures) would allow to observe the changes on the surface ''in status nascendi.'' Rather, it is important to stress that the interpretation of the measurements gets complicated due to the phenomena which occur in the process of heating and cooling. For this, consider the schematic defect chemistry diagram in Fig. 2. In our case, the conditions for preparation of the crystal are chosen in such a way as to provide reduction in the *n* regime, e.g., for a partial pressure of 10^{-8} Torr. However, the starting point for a preparation of the crystal at elevated temperature and, at the same time, the end point for the actual measurement after cooling, would be both situated on the ''hypothetical'' isotherm at room temperature lying actually in the *p* regime, and thus in

an oxidizing regime (the minimum of the ''hypothetical'' isotherm at room temperatures would lie below app. 10^{-30} Torr). Therefore the crystal is inevitably traversing the different regimes on heating and cooling and the surface will accordingly try to adjust to the different conditions.

Consider, for instance, a process where only a slow cooling is applied to a sample after reduction at elevated temperatures. In such a case, the reduced crystals would have time enough to equilibrate (at least near the surface) to the oxidizing conditions as the temperature decreases. In the case of only oxidizing a crystal this is not critical; the processes are additive on heating and cooling as the sample would stay within the *p* regime. In contrast, in the case of reduction the crystal is traversing the different regimes, and the two processes of reduction and oxidation may even counteract the redistribution of material within the surface region depending on the details of the heating and, for our argument more important, the cooling process. These considerations lie at the heart of the differences observed between our slow cooling and quenching experiments. The actual composition of the different chemical phases within the surface region can only be frozen in by quenching the reduced crystal. But notice, even in this case, segregation of material to the surface (Sr or SrO complexes) can occur. In fact, we attribute the appearance of the additional dropletlike structures on the surface of reduced crystals (see above and Ref. 17) to this redistribution of matter on cooling as the crystal tries to equilibrate to the conditions of the *p* regime. As pointed out in Ref. 17, it may also explain the enrichment of Sr right at the surface of reduced crystals as detected by SIMS even after quenching. Notice that these features are also apparent as clusters in the STM results by Refs. 25 and 28 and have been analyzed to consist indeed of SrO.[28] Interestingly enough, Jiang and Zegenhagen[25] noted that the density of such clusters increases after exposing to air and reannealing in UHV. This is understandable considering the nonadditive effects of redistribution of matter in the surface region as the samples crosses the borderline between *n* and *p* regime on heating and cooling. This in mind, the appearance of canyonlike structures observed in the experiments with a relatively slow cooling rate (see Figs. 6 and 7 and Ref. 28), in comparison with the situation after quenching, could then be explained by the redistribution of matter during the cooling process. In case sufficient time is available, the extra material may then be accommodated in the crystal structure on the surface, thus giving rise to microcrystals of an additional phase on and right underneath the surface. In fact, notice that the structures leading to the canyonlike features show indications of a regular arrangement with a preferential orientation. Such a regular organization and orientation along (100) is observed for the extended defects (see, e.g., Ref. 32 for $KNbO_3$). The reorganization on the surface with enough time may lead to the growth of additional crystal structures in other directions than perpendicular to the (100) orientation of the surface, which was the case of the oxidation process.

We conclude that the redistribution of matter and reorganization processes on heating and cooling lead to a complicated interplay of different phenomena. This way, the details of the preparation process, the history of the crystals in terms of previous thermal treatment, and the properties of the crystals concerning, e.g., the density of extended defects, influence the surface structure prepared at elevated temperatures. For instance, repeated reduction shows a tendency to build up a complicated surface structure with phases of both reducing and oxidizing origin. A case-in-point is the AFM pictures in Fig. 7 of a reduction at elevated temperatures proceeding in various steps on the same sample. These results indicate that such a complicated chemical restructuring may have to be taken into account in interpreting STM results for cases where crystals had been reduced in several thermal cycles with intermediate cooling. Therefore we would like to stress again that the dependence of the reorganization of the surface and in the surface region on the thermal history of crystals make it advisable to use always ''virgin'' crystals for the thermal preparation and employ quenching after reduction at elevated temperatures.

According to the arguments given above, we take the AFM measurements of the flash cooled samples (see Fig. 3) as a close representative for the topography of the reduced surface at elevated temperatures except for the appearance of dropletlike structures. The existence and growth of holes on the terraces of the surface is then taken as a signal of the loss of matter. Considering the restructuring of the near-surface region presented above [see Eq. (1)], several processes occur: SrO is depleted on and near the surface and oxygen is lost from exposed TiO_2 layers. Thermogravimetrical measurements and effusion experiments indicate only small losses of material from the samples for the temperature range chosen. We regard SrO as being the main component to be redistributed within the near-surface region. But, the TiO_2 layers exposed on the surface are subject to a further redistribution as a result of additional loss of surface oxygen. Turning to the characteristics of the terraces in our AFM results for (100) surfaces, we observed an increase in step height with temperature (see Table I in comparison with Table III) which we attribute to the appearance of Ti_2O and TiO layers on the surface.

Our results and interpretation for treatment of $SrTiO_3$ in reducing conditions at elevated temperatures suggests the enrichment of Ti-rich layers on the (100) surface or, within our framework, depletion of Sr and O. The fact that the surface of crystals annealed in ultrahigh vacuum becomes dominated by TiO_2-terminated layers had already been inferred from surface sensitive spectroscopy.[30] It is also well known that these layers are subject to the additional loss of oxygen, which introduces oxygen vacancies and causes dramatic changes in the electronic structure.[1,30] This loss of oxygen is readily apparent in photoemission data for surfaces of $SrTiO_3$ [see Refs. 4 and 30 for (100) surfaces, Refs. 26 and 65 for (110) surfaces, and Ref. 66 for (111) surfaces]. Experiments by scanning tunnel microscopy on (100) surfaces have indicated a vacancy ordering leading to various forms of reconstructions,[24–26] the details of which are highly dependent on annealing procedures and parameters.[25] Our results show that for the extensive thermal treatment applied in this work (annealing for 24 h) the effects on the surface go far beyond the introduction of vacancies and reconstruction. Since the restructuring of the reduced surfaces is better described by the formation of new Ti-rich phases, vacancy formation and ordering on the surface may then be regarded as an intermediate step or as a reconstruction of a surface already modified by the developing new chemical phases.

Moreover, the details of the heat treatment and cooling procedure clearly play a significant role. Our results point to the necessity to design experiments which allow to eliminate the opposing effects of the so-called *n*- and *p*-type nonstoichiometries invariably encountered during both heating and cooling.

Combining the available information, the observed changes in the morphology of the surface may then be rationalized in different steps. The depletion of SrO in the uppermost layers and continuous reduction of the exposed TiO_2 layers leads to an interesting thermodynamic state in the uppermost layers of the crystals. The uppermost layers are characterized by an extensive breaking of bonds for Ti. Correspondingly, Ti becomes more mobile on the surface. This, in turn, can lead to a diffusion of Ti with its remaining oxygen along the surface and causes the successive enlargement of the holes which are apparent in the AFM data as given in Fig. 3. Further reorganization results in a growth of the titanium-rich phases such as TiO and Ti_2O on the surface with their respective step heights (see Tables I and III).

D. Potential driving forces for a decomposition of the near-surface region of perovskite crystals

The theoretical interpretation of changes on the surface of perovskite crystals induced by thermal treatment have so far been limited to analysis in terms of relaxation, rumpling, reconstruction, and segregation. For instance, the modifications of the crystallographic geometry of the uppermost atomic layers and of the electronic structure at the surface have been described as an effect of changes in the Madelung potential on the surface.[67] Such models, which play an important role in the interpretation of the catalytic properties of perovskite crystals and have found support by theoretical calculations,[8] allow a description of the potential reorganization of only the uppermost monolayers. Similarly, the analysis of the enrichment or depletion of one of the cationic species on the surface by equilibrium segregation models (see, e.g., Refs. 68 and 36) applies to the uppermost layer or, at the most, a few atomic layers. However, the experimental evidence confronts us with a dramatic chemical reorganization of the near-surface region and a multilayer-type ordering. The only models developed in solid state science to account for such changes on a macroscopic scale in ternary oxides are based on kinetic demixing. In these models the driving forces for the solid-state reactions are connected to the differences in mobility of the involved cations under an applied gradient, either thermal (see, e.g., Ref. 69, and references therein), electrical (see, e.g., Ref. 70), mechanical (see, e.g., Ref. 71, and references therein), or chemical (see, e.g., Ref. 72, and references therein) in nature. Accordingly, crystals or ceramics of a ternary oxide of composition ABO_3 would decompose into the main binary oxides AO and BO_2 (Ref. 73) as well as, probably, a series of intermediate oxides such as $AO^*(ABO_3)_n$ and $AO^*(BO_2)_n$.[74] Without imposed gradients the original crystals are presumed to be chemically stable within a wide range of temperatures and partial pressure of oxygen (see, e.g., Ref. 73). For a perovskite of ABO_3 type such as $BaTiO_3$ the effect of kinetic demixing can be observed as a result of an applied electrical gradient.[42] Yet, the observed chemical restructuring on the surface and in the near-surface region of $SrTiO_3$ as described above is found for isothermal and isobaric conditions. And, the crystals under investigation are not subjected to externally imposed electrical fields or mechanical stress. Therefore kinetic demixing does not seem to apply directly to the situation encountered in our kind of experiment. On the other hand, one may not neglect minimal thermal gradient between the bulk and the surface of samples as a result of dynamical heating procedures. But, we have convinced ourselves that the dynamics of the restructuring depends critically on the duration of the high-temperature treatment (see, e.g., Fig. 12) as long as heating and cooling rates are similarly large.

Without external gradients, the observed decomposition in $SrTiO_3$ can only be understood by assuming internal fields, either electrical or mechanical in nature, between the bulk and the surface of the crystal, or by considering the perovskite as a metastable chemical phase. In fact, the latter becomes highly relevant for $SrTiO_3$ for temperatures above 1000 °C. By thermogravimetrical measurements of undoped stoichiometric single crystals (and also donator doped crystal) in dry oxygen (synthetic air, $p_{O_2} \approx 200$ Torr) we observed the onset of loss of material at app. 1000 °C. Just above 1000 °C the loss of material becomes substantial amounting to app. 0.05%. Our analysis of the evaporated species on the basis of fluorescence spectroscopy (characterizing the material deposited opposite the sample) revealed that this consisted of mainly strontium. This then implies that the evaporation of Sr or Sr oxides are driving forces for a decomposition of the perovskite at such high temperatures. In this case, the defect chemistry can only be described within a three-dimensional space, where both the activity of O_2 as well as surrounding strontium are independently varied.

Returning to the important issue of the kind of driving forces responsible for the decomposition for temperatures below 1000 °C without a preferential evaporation or loss of material brings the role of extended defects in the perovskite into focus. For $SrTiO_3$, Wang *et al.*[75] have very recently shown that the density of dislocations is unusually high in ''skin'' region of originally cut single crystals. These extended defects do not only act as fast diffusion paths for a redistribution of the cations, predominantly Sr, within the near-surface region (see above), but are accompanied by a strained region. This may be sufficient for the local mechanical stress gradients (nanostress) to act as driving force for the segregation of cations. Indeed, elasticity-induced solute redistribution around dislocations have been discussed in the literature (see, e.g., Ref. 71, and references therein). An illustration of the effect of the mechanical forces imposed on $SrTiO_3$ at elevated temperatures (here 1000 °C) can be taken from Fig. 13. It is well known that single-crystalline $SrTiO_3$ show plastic deformation at elevated temperatures.[76–78] The surface of those parts of the crystals with maximum mechanical strain do not only reveal the above analyzed step-terrace formation with 6 or 12 Å but also the growth of microcrystals. The dimension of these additional microcrystals is correlated to the bending curvature of single crystals [compare Figs. 13(b) and 13(c)]. Outside the main strained parts of the crystals no microcrystals are observed leaving only the characteristic steplike terraces [compare Fig. 13(a) with Fig. 3(a)]. This result demonstrates that mechanical

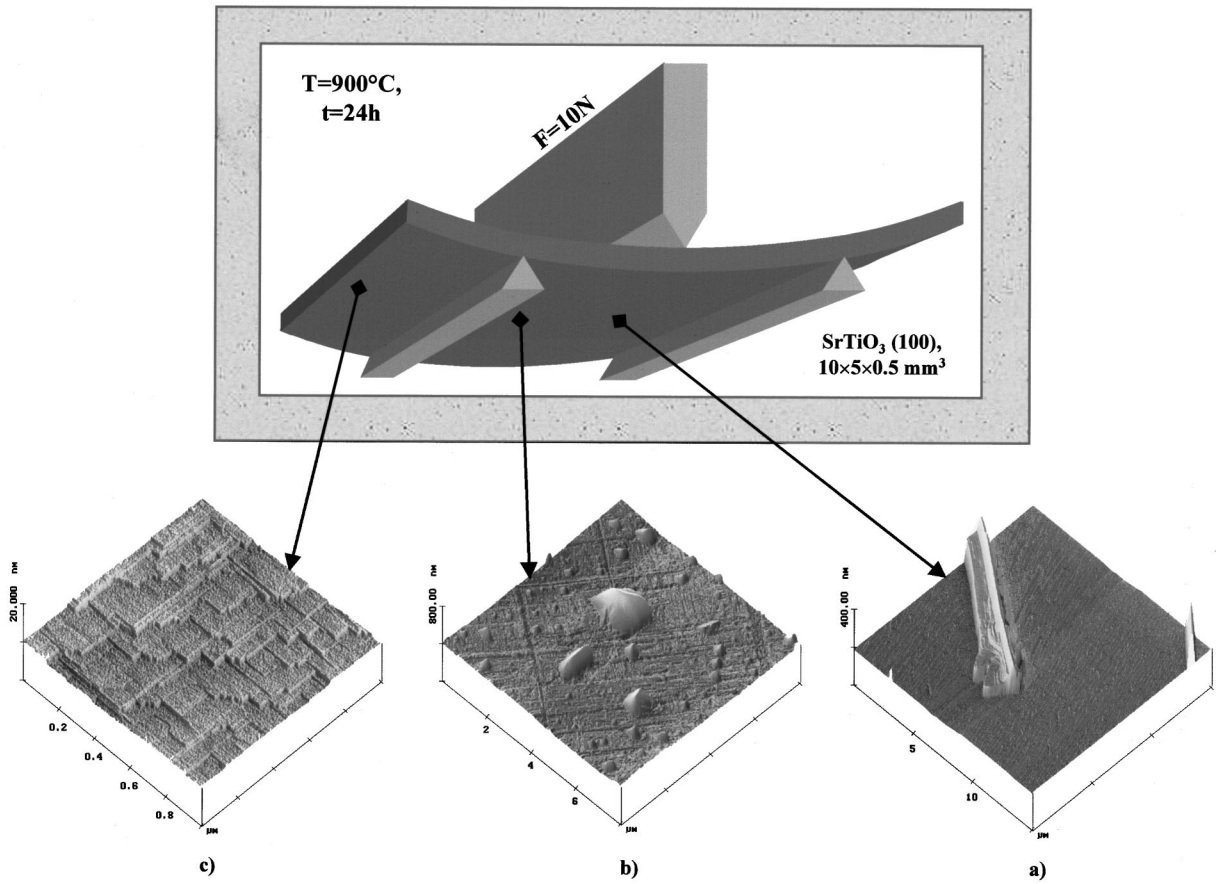

FIG. 13. AFM measurements of a $SrTiO_3$ crystal with (100) orientation mechanically deformed at 900 °C for 24 h. (a) and (b) correspond to regions of the crystal with high deformation, whereas (c) shows a portion of the crystal with small strain. The whole surface is covered with the kind of steplike terraces characteristic for these temperatures [see also Fig. 3(a)]. In addition, the deformation zone exhibits the formation of microcrystals as a result of a massive redistribution of material and subsequent recrystallization.

stress leads to a massive segregation of extra material and subsequent recrystallization. Further analysis of the composition by electron microprobe gives evidence of the accumulation of Sr. It is also interesting to note that we observed a similar behavior concerning the growth of microcrystals at elevated temperatures for strained surfaces as a result of roughening or scratching at room temperature.

A note should be added concerning the important role of the accompanying shearing mechanism on a macroscopic scale involved in the high-temperature restructuring. This is important since the segregation and subsequent intercalation of material, here SrO, should, in principle, lead in the laboratory framework to an increase of the dimension of the crystal and thus to an increase in the mechanical energy and internal mechanical strain. Yet, the optimal restructuring, which does not involve any appreciable change in dimension, should rely on the shearing mechanism between dismantled, or deintercalated, layers (compare with Fig. 11). The effect of shearing mechanisms in the perovskite accompanying AO depletion is documented in the literature.[79,80]

The driving forces for redistribution of the cations in presence of extended defects may not only be due the strained region around extended defects but, in addition, may arise by differences in the formation energy of defects between the extended defects and the bulk of the crystal, just like discussed in the literature for the surface segregation between the surface and the bulk (see, e.g., Refs. 36 and 68, and references therein). Yet, very little information is available for such formation energies. For $SrTiO_3$ only bulk values have been theoretically calculated indicating the energetic preference of Schottky-like SrO vacancies.[58] Along this line of argument the extended defects act as an internal source of Sr and SrO complexes. Yet, as already pointed out by Liang and Bonnell,[29] the kind of modifications encountered give rise to dramatic spatial variations and very different chemical surroundings and thus make it more appropriate to consider the equilization of chemical activities as acting driving forces rather than differences in defect formation energies.

Discussing the potential driving forces for the restructuring in the near-surface region the influence of space charge effects has to be considered (concerning the possible role of such effects in the case of $SrTiO_3$, see Refs. 68, 36, and 29). We have therefore set out to measure the potential difference as a result of the restructuring of the near-surface region. Yet, one does not succeed to measure a potential difference directly on crystals subjected to heat treatment. The shell-like structure of the inhomogeneous near-surface region around the crystal (see Fig. 10) does not produce a voltage between the outer electrodes on opposite sides of the crystal since the different potential differences are oriented against each other. On the other hand, it becomes easily detectable for heat-treated crystals (here 1000 °C) after fracturing or

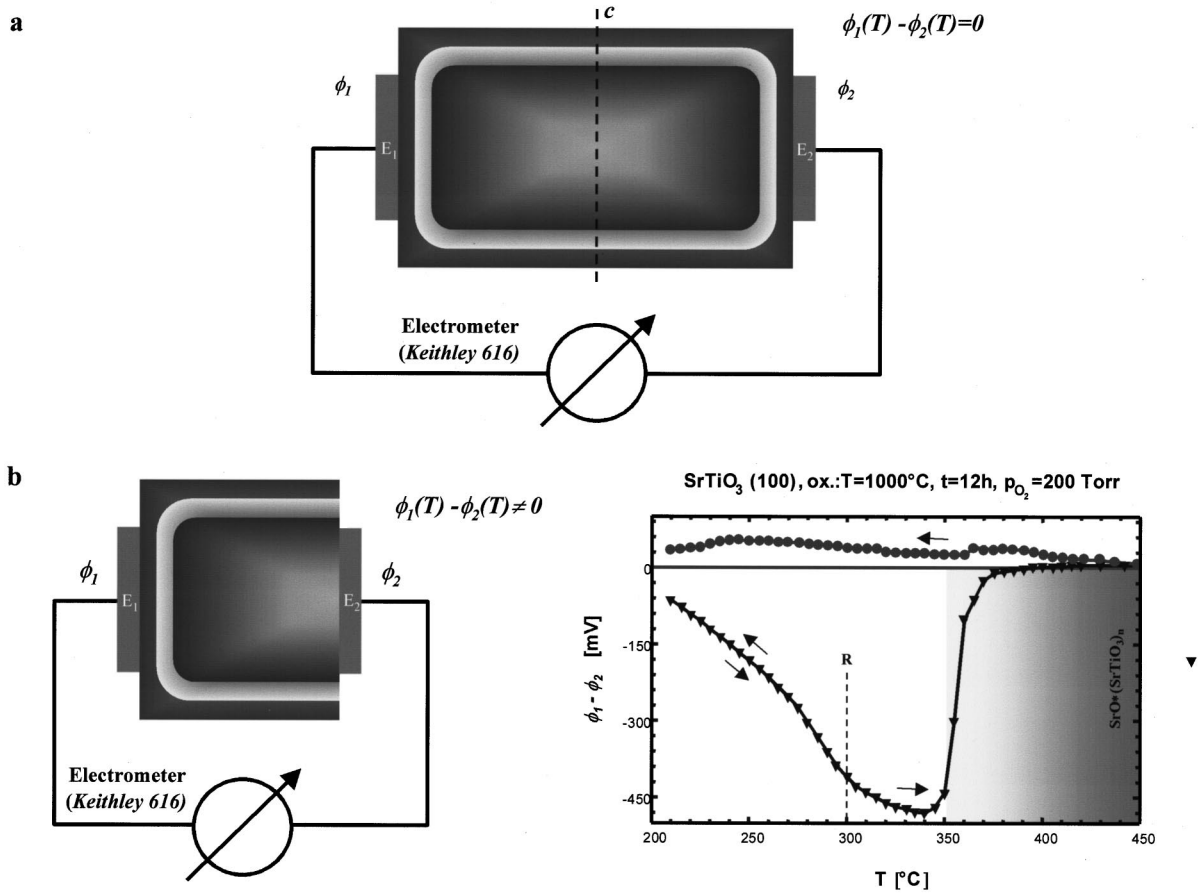

FIG. 14. Measurement of the potential difference of a single crystal prepared for 24 h at 1000 °C in oxidizing conditions. Negligible potential difference is measured for the shell-like configuration of the inhomogeneous near-surface region [symmetrical configuration visualized in (a)]. For an asymmetrical configuration [see (b)] a large potential difference can de detected which shows a reversible behavior as a function of temperature up to app. 300 °C (indicated by R). Above this temperature, the potential difference exhibits a totally different behavior for the heating and cooling cycle (given by the arrows) as a result of the restoration of a symmetrical configuration. We assume that the potential difference is related to the concentration gradient for Sr within the near-surface region:

(a) $E1|\mathrm{SrO}|\mathrm{SrO}\times(\mathrm{SrTiO_3})_n|\mathrm{TiO_2}|\mathrm{SrTiO_3}|\mathrm{SrO}\times(\mathrm{SrTiO_3})_n|\mathrm{SrO}|E2$
$\varphi_{E1}-\varphi_{E2}=0, \quad E1=E2$ (Au, Ag)

(b) $E1|\mathrm{SrO}|\mathrm{SrO}\times(\mathrm{SrTiO_3})_n|\mathrm{TiO_2}|\mathrm{SrTiO_3}|E2$
$\varphi_{E1}-\varphi_{E2}\neq 0, \quad E1=E2$ (Au, Ag).

removal of the inhomogeneous near-surface region on one side of the sample, thus producing an assymmetrical configuration (see Fig. 14). The observed values are dependent on temperature reaching a maximum (of app. 500 meV) around 330–340 °C and are reversible for repeated measurement. The surface is found to be negatively charged with respect to the bulk and thus opposite in sign compared to the kind of space charge potential as predicted, for example, by Desu and Paine for $BaTiO_3$ (Ref. 68, but see Nowotny in Ref. 81). Even more, the values are much larger as anticipated and are electrochemical in origin. The measured potential difference is due to a diffusion of Sr ions within the near-surface region as a result of the imposed concentration gradient in this region of the crystal at high temperatures. In this respect it is even tempting to consider the multilayer-type heterogeneity within the near-surface region with the intercalated (RP phase) and deintercalated (TiO_2) material as a local analog of a rocking-chair battery (see, e.g., Julien in Ref. 81). The mobility of Sr ions at low temperatures is not surprising in view of the high Sr leaching rate observed for $SrTiO_3$ at these temperatures (below 300 °C) (Ref. 82) or the processes involved in hydrothermal preparation (at 120–220 °C) of $Sr_3Ti_2O_7$-$SrTiO_3$ microcomposite particles with an epitaxial core-shell structure.[83] Such high mobility of *A* cations, even in absence of aqueous solutions, are known in ternary oxides. Na_xWO_3 serves as a particular impressive case in point for the unusual high cationic mobility at low temperatures due to the movement of Na along channels (see, e.g., Ref. 84, and references therein). We would also like to emphasize that measurements of the potential difference is an established procedure to analyze the kinetics of ion migration for ternary oxides (see, e.g., Ries and Schoonman in Ref. 81). Above 350 °C our measurement shows a completely different behavior compared to low temperatures. For instance, the observed potential difference decreases dramatically with temperature with a remaining potential difference in the order of only a few mV. And, the measurement is irreversible as the potential difference does not regain either its original values nor its temperature dependence. We therefore conclude that a restoration of a symmetrical electrochemical configuration (shell structure surrounding the crystal) sets in at temperatures above 350 °C. Interestingly enough, this temperature

coincides with the temperature necessary to induce the solid phase reactions and A^{++} diffusion in the combination reactions of $PbO+TiO_2$ for synthesis of $PbTiO_3$ (see, e.g., Ref. 85, and references therein). In our view, the processes at these temperatures cannot be directly compared the situation encountered at high temperature, but have to be regarded as a precursor of the kind of the high-temperature chemical restructuring.

Considering the intercalation and deintercalation mechanism further studies are necessary to unravel the details of the processes involved. Some microscopic information concerning the deintercalation can be already taken from geological investigations on natural perovskite[79] and concerning the intercalation mechanism we refer to, e.g., Refs. 50 and 53.

Our analysis of the potential driving forces and the role of the extended defects has so far concentrated on oxidizing conditions. For reducing conditions we know that the sequence of intercalation and deintercalation is in an opposite order and also involves the extended defects. Yet, we cannot transfer our arguments concerning the driving forces directly since the situation is more complicated with the influence of the induced oxygen deficiency on the transport properties of the extended defects, the local stress fields as well as the defect formation energies.

Finally, it should be pointed out that the relationship between the high-temperature behavior and kinetic demixing put forward for $SrTiO_3$ in the present study has also been discussed for doped binary oxides. Just like in our case, doped binary oxides showed kinetic demixinglike phenomena though the crystals were not subjected to any external gradient but only abrupt changes of one of the thermodynamical variables, either partial pressure of oxygen (see, e.g., Ref. 86) or temperature (see, e.g., Ref. 87).

V. SUMMARY

Summarizing our results, the topographical and structural information provide an interesting picture of the character of the real surface of $SrTiO_3$ after extensive thermal treatment for temperatures in the range of 800–1000 °C. We observed a dramatic restructuring for both reducing and oxidizing conditions leading to the formation of nonperovskite phases on the surface. For oxidized crystals with (100) orientation, this caused the formation of a regular SrO-rich surface with the Ruddlesden-Popper phase Sr_2TiO_4 [$SrO^*(SrTiO_3)n$ with $n=1$] above 900 °C. The formation of regular terraces with a step height of app. 11.8 Å was observed, which may enhance the quality of $SrTiO_3$ as substrate for specific high-T_c superconductors. For the reduced state, we concluded that the restructuring of the surface region leads to the formation of a Ti-rich phase of type TiO and Ti_2O on the surface above 900 °C, depending on the reduction level.

The modifications of the surface are a manifestation of the restructuring in the near-surface region which leads to a chemically heterogeneous ''skin'' in the case of $SrTiO_3$. This restructuring is attributed to a kinetic demixinglike behavior at elevated temperatures. Even more, the crystals cannot be regarded to be equilibrated for the preparation conditions employed. In fact, evidence is given that the surface undergoes a continuous change in time, which, in the case of oxidizing conditions, leads to a continuous accumulation of SrO on the surface and, in the case of reducing conditions, to the ongoing loss of oxygen from the Ti-enriched surfaces. We argue that the extended defects play an important role in the restructuring of the near-surface region. The local strain fields in the neighborhood of the extended defects and equalization of chemical activities are put forward as possible driving forces for the kinetic demixinglike behavior.

The presented results indicate the importance of the details of the preparation process, the history of the crystals in terms of the thermal treatment and their defect characteristics, especially the existence of extended defects. Our analysis forms the basis for more complicated heat treatment procedures which by combination of processes may induce topographical changes with special features (see, e.g., Refs. 27 and 88).

Our study has been confined to the (100) and (110) surfaces of undoped $SrTiO_3$. It would be interesting to study the polar surfaces such as (111) in a similar way in order to extend the analysis of Refs. 89 and 90. Also, the effect of doping on the properties of the surface should be investigated, in particular, the introduction of donators by either Sr or Ti substitution, e.g., by La or Nb, respectively, and corresponding structural changes induced by the oxidative nonstoichiometry in these systems (see, e.g., Refs. 91 and 92).

We argue that the results for $SrTiO_3$ can be generalized to the whole class of perovskites of ABO_3 type. For this, systematic AFM studies for a whole series of other perovskite including $BaTiO_3$, $KNbO_3$, and $KTaO_3$ are currently under way. It should be pointed out that the model presented, which emphasizes the role of the extended defects and the formation of a chemical heterogeneity near to and on the surface, provides a shift of focus of the defect chemistry of the ABO_3 perovskites. One is confronted for these perovskite with a situation very similar to the case of binary oxides, such as oxygen deficient TiO_2, where the nonstoichiometry is not governed by classical point defect chemistry, but, instead, governed by ordered superstructures and corresponding crystallographic shearing mechanisms.

ACKNOWLEDGMENTS

One of us (K.S.) would like to thank the Forschungszentrum Jülich for financial support and for the possibility to work in a stimulating interdisciplinary environment. We want especially to acknowledge J. Herion who supported our project and gave us the opportunity to perform *in situ* measurements. Furthermore, we would like to thank R. Waser for extensive discussions on the defect chemistry of perovskite.

*Permanent address: Institute of Physics, Silesian University, PL 40-007 Katowice, Poland. Present address: Institut für Festkörperforschung, Forschungszentrum Jülich, D-52425 Jülich, Germany.

[1] V. E. Henrich and P. A. Cox, *The Surface Science of Metal Oxides* (Cambridge University Press, Cambridge, England, 1994).
[2] C. Noguera, *Physics and Chemistry at Oxide Surfaces* (Cam-

bridge University Press, Cambridge, England, 1995).
[3] F. M. F. de Groot, J. Faber, J. J. Michiels, M. T. Czyzyk, M. Abbate, and J. C. Fuggle, Phys. Rev. B **48**, 2074 (1993); O. V. Krasovska, E. E. Krasovskii, and V. N. Antonov, Solid State Commun. **97**, 1019 (1996); H. Haruyama, S. Kodeira, Y. Aiura, H. Bando, Y. Nishihara, T. Maruyama, Y. Sakisaka, and H. Kato, Phys. Rev. B **53**, 8032 (1996).
[4] V. E. Henrich, G. Dresselhaus, and H. J. Zeiger, Phys. Rev. B **17**, 4908 (1978); V. E. Henrich, Prog. Surf. Sci. **14**, 175 (1983); R. Courths, J. Noffke, H. Wern, and R. Heise, Phys. Rev. B **42**, 9127 (1990).
[5] V. Ravikumar, D. Wolf, and V. P. David, Phys. Rev. Lett. **74**, 960 (1995).
[6] S. Kimura, J. Yamauchi, M. Tsukada, and S. Watanabe, Phys. Rev. B **51**, 11049 (1995).
[7] H.-B. Neumann, U. Rütt, J. R. Schneider, and G. Shirane, Phys. Rev. B **52**, 3981 (1995).
[8] T. Wolfram and S. Ellialtioglu, in *Theory of Chemisorption*, edited by J. R. Smith (Springer-Verlag, Berlin, 1980), p. 149.
[9] V. C. Matijasevic, B. Ilge, B. Stäuble-Pümpin, G. Rietveld, F. Tuinstra, and J. E. Moorij, Phys. Rev. Lett. **76**, 4765 (1996).
[10] Yu. A. Boikov, Z. G. Ivanov, A. N. Kiselev, E. Olsson, and T. Claeson, J. Appl. Phys. **78**, 4591 (1995); Yu. A. Boikov and T. Claeson, *ibid.* **81**, 3232 (1997).
[11] A. Raith, P. Reijnen, and R. Waser, Ber. Bunsenges. Phys. Chem. **92**, 1516 (1988).
[12] R. Stumpe, D. Wagner, and P. Bäuerle, Phys. Status Solidi A **75**, 143 (1983).
[13] J. F. Schooley, W. R. Hosler, and M. L. Cohen, Phys. Rev. Lett. **12**, 474 (1964).
[14] G. Binnig and H. E. Hönig, Solid State Commun. **14**, 597 (1974).
[15] H. Yamada and G. R. Miller, J. Solid State Chem. **6**, 169 (1973).
[16] R. Waser and D. M. Smyth, in *Ferroelectric Thin Films: Synthesis and Basic Properties* (Gordon and Breach, New York, 1994), p. 584.
[17] K. Szot, W. Speier, J. Herion, and Ch. Freiburg, Appl. Phys. A: Mater. Sci. Process. **64**, 55 (1997).
[18] S. N. Ruddlesden and P. Popper, Acta Crystallogr. **10**, 538 (1957); **11**, 54 (1958); but see also M. Drys and W. Trzebiatowski, Rocz. Chem. **31**, 489 (1957); K. Lukaszewicz, Anal. Chem. **70**, 320 (1958); Rocz. Chem. **33**, 239 (1959).
[19] J. P. LaFemina, Crit. Rev. Surf. Chem. **3**, 297 (1994).
[20] D. A. Bonnell, Prog. Surf. Sci. **57**, 187 (1998).
[21] T. Hikita, T. Hanada, and M. Kudo, Surf. Sci. **287/288**, 377 (1993).
[22] M. Kawasaki, K. Takahashi, T. Maeda, R. Tsuchiya, M. Shinohara, O. Isiyama, T. Yonezawa, M. Yoshimoto, and H. Koinuma, Science **266**, 1540 (1994).
[23] B. Cord and R. Courths, Surf. Sci. **162**, 34 (1985).
[24] T. Matsumoto, H. Tanaka, T. Kawai, and S. Kawai, Surf. Sci. Lett. **278**, L153 (1992); T. Matsumoto, H. Tanaka, K. Kouguchi, T. Kawai, and S. Kawai, Jpn. J. Appl. Phys., Part 1 **32**, 1405 (1992); T. Matsumoto, H. Tanaka, K. Kouguchi, T. Kawai, and S. Kawai, Surf. Sci. **312**, 21 (1994); H. Tanaka, T. Matsumoto, T. Kawai, and S. Kawai, *ibid.* **318**, 29 (1994).
[25] Q. D. Jiang and J. Zegenhagen, Surf. Sci. Lett. **338**, L882 (1995).
[26] H. Bando, Y. Aiura, Y. Haruyama, T. Shimizu, and Y. Nishihara, J. Vac. Sci. Technol. B **13**, 1150 (1995).
[27] Q. D. Jiang and J. Zegenhagen, Surf. Sci. **367**, L42 (1996).
[28] Y. Liang and D. A. Bonnell, Surf. Sci. Lett. **285**, L510 (1993); Y. Liang and D. A. Bonnell, Surf. Sci. **310**, 128 (1994).
[29] Y. Liang and D. A. Bonnell, J. Am. Ceram. Soc. **78**, 2633 (1995).
[30] A. Hirata, A. Ando, K. Saiki, and A. Koma, Surf. Sci. **310**, 89 (1994); A. Hirata, K. Saiki, A. Koma, and A. Ando, *ibid.* **319**, 267 (1994).
[31] T. Nishimura, A. Ikeda, H. Namba, T. Morishita, and Y. Kido, Surf. Sci. **421**, 273 (1999).
[32] K. Szot, W. Speier, S. Cramm, J. Herion, Ch. Freiburg, R. Waser, M. Pawelczyk, and W. Eberhardt, J. Phys. Chem. Solids **57**, 1765 (1996).
[33] E. S. Hellmann, D. G. Schlom, N. Missert, K. Char, J. S. Harris, M. R. Beasley, A. Kapitulnik, T. H. Geballe, J. N. Eckstein, S.-L. Wenig, and C. Webb, J. Vac. Sci. Technol. B **6**, 799 (1988).
[34] M. Naito and H. Sato, Physica C **229**, 1 (1994).
[35] T. Nakamura, H. Inada, and M. Iiyama, Jpn. J. Appl. Phys., Part 1 **36**, 90 (1997).
[36] G. Horvath, J. Gerblinger, H. Meixner, and J. Giber, Sens. Actuators B **32**, 93 (1996).
[37] R. Sum, R. Lüthi, H. P. Lang, and H.-J. Güntherodt, Physica C **235**, 621 (1994); R. Sum, H. P. Lang, and H.-J. Güntherodt, *ibid.* **242**, 174 (1995).
[38] B. Stäuble-Pümpin, B. Ilge, V. C. Matijasevic, P. M. L. O. Scholte, A. J. Steinfort, and F. Tuinstra, Surf. Sci. **369**, 313 (1996).
[39] I. Kawayama, M. Kanai, and T. Kawai, Jpn. J. Appl. Phys., Part 2 **35**, L926 (1996).
[40] N. Ikemiya, A. Kitamura, and S. Hara, J. Cryst. Growth **160**, 104 (1996).
[41] S. S. Sheiko, M. Möller, E. M. C. M. Reuvekamp, and H. W. Zandbergen, Phys. Rev. B **48**, 5675 (1993).
[42] K. Szot, M. Pawelczyk, J. Herion, Ch. Freiburg, J. Albers, R. Waser, J. Hulliger, J. Kwapulinski, and J. Dec, Appl. Phys. A: Mater. Sci. Process. **62**, 335 (1996).
[43] R. Moos, Ph.D. thesis, Karlsruhe, 1994; Fortschritt-Berichte Series 5, No. 362, VDI-Verlag, Düsseldorf, 1994 (in German).
[44] A. E. Palladino, J. Am. Chem. Soc. **48**, 478 (1965).
[45] A. M. J. H. Seuter, Philips Research Reports, Supplement No. 3, 1974 (unpublished).
[46] O. Sarid, *Scanning Force Microscopy* (Oxford University, New York, 1994).
[47] D. M. Smyth, Annu. Rev. Mater. Sci. **15**, 329 (1985).
[48] R. J. D. Tilley, *Defect Crystal Chemistry* (Blackie, Glasgow, 1987).
[49] The formation of an oxygen-deficient phase (Magnéli-type structures Ti_mO_{2m-1}) under oxidizing conditions is somewhat surprising. In order to provide an adequate description one may have to either include the loss of oxygen (unrealistic) or a segregation of SrO_2. Including the segregation of SrO (see also Sec. IV B) and SrO_2 as well as the uptake of oxygen Eq. (2) could be extended as follows:

$$k\times SrTiO_3+s\times\tfrac{1}{2}O_2\downarrow\leftrightarrow p\times SrTiO_3+q\times SrO^*(SrTiO_3)_n+u\times SrO+w\times TiO_2+t\times SrO_2+l\times Ti_mO_{2m-1} \quad (3)$$

$$k=p+q\times(n+1)+u+t,\ n\in\langle 1\text{–}10\rangle,\ w=u+q,\ t=l\times m,\ s=l\times(m-1),\ m\in\langle 2\text{–}50\rangle.$$

But notice that the melting temperature of SrO_2 is around 700–800 °C, which makes such a reaction rather improbable.
[50] R. J. D. Tilley, J. Solid State Chem. **21**, 293 (1977).
[51] K. R. Udayakumar and A. N. Cormack, J. Am. Chem. Soc. **71**, C469 (1988).

[52] K. Hawkins and T. J. White, Philos. Trans. R. Soc. London, Ser. A **336**, 541 (1991).
[53] M. A. McCoy, R. W. Grimes, and W. E. Lee, Philos. Mag. A **75**, 833 (1997).
[54] M. Fujimoto and M. Watanabe, J. Mater. Sci. **20**, 3683 (1985).
[55] N. G. Eror and U. Balachandran, J. Solid State Chem. **42**, 227 (1982); U. Balachandran and N. G. Eror, J. Mater. Sci. **17**, 2133 (1982); S. Witke, D. M. Smyth, and H. Pickup, J. Am. Ceram. Soc. **67**, 372 (1984); Y. H. Han, M. P. Harmer, Y. H. Hu, and D. M. Smyth, in *Transport in Nonstoichiometric Compounds*, Vol. 129 of *NATO-ASI, Series B: Physics*, edited by G. Simkovich and V. S. Stubican (Plenum, New York, 1984), p. 73.
[56] M. Pawelczyk (unpublished).
[57] V. V. Prisedskii and Y. D. Tret'yakov, Inorg. Mater. **18**, 1926 (1982).
[58] M. J. Akhtar, Z.-U.-N. Akhtar, R. Jackson, and C. R. A. Catlow, J. Am. Ceram. Soc. **78**, 421 (1995) have calculated that ''Schottky-like'' SrO defects are the energetically favorable defects in $SrTiO_3$ and proposed from a theoretical point of view a Sr deficiency at elevated temperatures.
[59] I. Sakaguchi and H. Haneda, J. Solid State Chem. **124**, 195 (1996).
[60] The tracer experiments (reoxidation with ^{18}O after thermal reduction) in combination with SIMS depth profiling in the case of $SrTiO_3$ did not allow to extract reliable information on the high diffusion paths since the ^{18}O signal for deep penetration (above 10 μm) turned out to be of the order the background level due to the natural abundance of this isotope. But note that the desorption rate of oxygen is less than $10^{12}\,cm^{-2}\,s^{-1}$ as determined by thermal desorption spectroscopy in reducing conditions, which was well below the oxygen exchange rate between the samples and ^{18}O atmosphere in our tracer experiments; U. Zastrow, K. Szot, M. Beyer, and W. Speier, in *SIMS XI*, edited by G. Gillen, R. Lareau, J. Bennett, and F. Stevie (John Wiley & Sons, Chichester, 1998), p. 393.
[61] L. A. Bursill, J. Peng, and X. Fan, Ferroelectrics **97**, 71 (1989).
[62] T. Williams, F. Lichtenberg, D. Widmer, J. G. Bednorz, and A. Reller, J. Solid State Chem. **103**, 375 (1993).
[63] K. Szot, W. Speier, and W. Eberhardt, Appl. Phys. Lett. **60**, 1190 (1992).
[64] K. Szot, W. Speier, U. Breuer, R. Meyer, and R. Waser (unpublished).
[65] Y. Aiura, H. Bando, Y. Nishihara, Y. Haruyama, S. Kodaira, T. Komeda, Y. Sakisaka, T. Maruyama, and H. Kato, in *Advances in Superconductivity VI*, edited by T. Fujita and Y. Shiohara (Springer-Verlag, Tokyo, 1994), p. 983.
[66] W. J. Lo and G. A. Somorjai, Phys. Rev. B **17**, 4942 (1978).
[67] R. Courths, J. Noffke, H. Wern, and R. Heise, Phys. Rev. B **42**, 9127 (1990).
[68] S. B. Desu and D. A. Payne, J. Am. Chem. Soc. **73**, 3391 (1990); **73**, 3398 (1990).
[69] D. Monceau, C. Petot, and G. Petot Ervas, J. Eur. Ceram. Soc. **9**, 193 (1992).
[70] W. T. Petuskey, J. Am. Ceram. Soc. **68**, 86 (1985).
[71] C. Reinke and W. C. Johnson, J. Am. Ceram. Soc. **78**, 2593 (1995).
[72] D. Monceau, C. Petot, and G. Petot Ervas, Solid State Ionics **45**, 231 (1991).
[73] W. Laqua and H. Schmalzried, in *Materials Science Monographs, 10:Reactivity in Solids*, Vol 1, edited by K. Dyrek, J. Haber, and J. Nowotny (Elsevier, Amsterdam, 1982), p. 194.
[74] G. Yamaguchi and T. Tokuda, Bull. Chem. Soc. Jpn. **40**, 843 (1967).
[75] R. Wang, Y. Zhu, and S. M. Shapiro, Phys. Rev. Lett. **80**, 2370 (1998).
[76] J. Nishigaki, K. Kuroda, and H. Saka, Phys. Status Solidi A **128**, 319 (1991).
[77] Z. Wang, S. Karato, and K. Fujino, Phys. Earth Planet. Inter. **79**, 299 (1993).
[78] H. Koizumi, S. Katakury, T. Suzuki, T. Yamamoto, and T. Sakuma, in *Strength of Materials*, edited by Oikawa *et al.* (The Japan Institute of Metals, Tokyo, 1994), p. 737.
[79] J. F. Banfield and D. R. Veblen, Am. Mineral. **17**, 545 (1992).
[80] V. V. Prisedskii, V. P. Komarov, G. F. Pan'ko, and V. V. Klimov, Ferroelectrics **23**, 23 (1980); for further references see Ref. 57.
[81] *Solid State Electrochemistry*, edited by P. J. Gellings and H. J. M. Bouwmeester (CRC Press, New York, 1997).
[82] H. W. Nesbitt, G. M. Bancroft, W. S. Fyfe, S. N. Karkhanis, A. Nishijima, and S. Shin, Nature (London) **289**, 358 (1981).
[83] T. Takeuchi, T. Tani, and T. Satoh, Solid State Ionics **108**, 67 (1998).
[84] T. Kudo and K. Fueki, *Solid State Ionics* (Kodansha, Tokyo, 1990).
[85] Y. Xu, *Ferroelectric Materials and Their Application* (North-Holland, Amsterdam, 1991), p. 115.
[86] J. A. S. Ikeda, Y.-M. Chiang, and B. Fabes, J. Am. Ceram. Soc. **73**, 1633 (1990).
[87] G. P. Ervas, C. Perot, and D. Monceau, J. Am. Ceram. Soc. **78**, 2314 (1995).
[88] Q. D. Jiang, X. Q. Pan, and J. Zegenhagen, Phys. Rev. B **56**, 6947 (1997).
[89] W. M. Sigmund, M. Rotov, Q. D. Jiang, J. Brunen, J. Zegenhagen, and F. Aldinger, Appl. Phys. A: Mater. Sci. Process. **64**, 219 (1997).
[90] H. Tanaka and T. Kawai, Surf. Sci. **365**, 437 (1996).
[91] M. E. Bowden, D. A. Jefferson, and I. W. M. Brown, J. Solid State Chem. **117**, 88 (1995); **119**, 412 (1995).
[92] D. M. Smyth, in *Properties and Applications of Perovskite-type Oxides*, edited by L. G. Tejuca and J. L. G. Fierro (Marcel Dekker, Inc., New York, 1993), p. 47.
[93] *Crystal and Solid State Physics*, edited by K.-H. Hellwege and A. M. Hellwege, Landolt-Börnstein, Group III Vol. 7, Pt. b (Springer-Verlag, Berlin, 1975).